Geosystems and Geoenvironment 2 (2023) 100188

Contents lists available at ScienceDirect

Geosystems and Geoenvironment

journal homepage: www.elsevier.com/locate/geogeo

Tectonic and metallogenic implications of W-Sn related granitoid rocks in the Kawthaung-Bankachon area, southernmost part of Myanmar: Constraints from petrology, geochemistry, and U-Pb zircon geochronology

Zin Mar Oo[a], Khin Zaw[b], Ivan Belousov[b], Prinya Putthapiban[c], Charles Makoundi[b,*]

[a] Department of Geology, Mawlamyine University, Mon State 12012, Myanmar
[b] CODES Centre for Ore Deposit and Earth Sciences, University of Tasmania, Private Bag 126, Hobart, Tasmania 7001, Australia
[c] Geoscience, Mahidol University, Kanchanaburi Campus, Kanchanaburi 71150, Thailand

ARTICLE INFO

Article history:
Received 6 September 2022
Revised 2 January 2023
Accepted 2 February 2023

Handling Editor: Vinod Samuel

Keywords:
Tectonics
Metallogenic implications
W-Sn related granitoid rocks
Zircon geochronology
Myanmar Terrane

ABSTRACT

Granitoid rocks are widely distributed along the N-S trending tectonic belts encompassing Myanmar, Thailand, Peninsular Malaysia, and Indonesia and these granitoid rocks are host to the world's largest deposits of tin-tungsten, in terms of both production and reserves. The investigated study area belongs to the southernmost part of the Central Cretaceous-Eocene granitoid belt of SE Asia in the border region of Myanmar and Thailand within the Sibumasu or Shan-Thai Terrane. The granitoid units in the area are biotite granite, muscovite-biotite granite, porphyritic biotite granite, and diorite which occur locally as dykes. All granitic rocks in the area are recognized in the High-K calc-alkaline series and show a high abundance of Cs, Rb, U, Th, K, Pb, Nd, Zr, and Sn. Based on the major oxide composition and tectonic discrimination diagram, all granitoid rocks in the area fall in the peraluminous, S-type granite category and within the Post-Orogenic Granite and Post-Collisional Granite fields. Radiometric dating by LA ICP-MS U-Pb zircon method yielded the ages of 78.97 ± 0.63 Ma (biotite granite), 79.59 ± 0.76 Ma (muscovite-biotite granite), and 79.14 ± 0.91 Ma (porphyritic biotite granite) and 49.48 ± 0.83 Ma for the biotite granite from the Yadanabon W-Sn deposit. According to the zircon U-Pb ages, the timing of the granitoid intrusions of the Kawthaung-Bankachon area is the Campanian (Late Cretaceous) to Eocene. The magmatism and W-Sn mineralization in the area is attributable to the Indian Ocean subduction and collision between the west Myanmar Terrane and the Sibumasu Terrane.

1. Introduction

Granitoid rocks are widely distributed in Myanmar and commonly associated with abundant lead, zinc, copper, tin, tungsten, and REE mineralization (e.g., Gardiner et al., 2015a, 2015b, 2016a, 2016b, 2017; Zaw, 1990, 2017). In recent years, several geological, geochemical, and U-Pb isotopic age dating on granitoid rocks in Myanmar and their tectonic and metallogenic relations were increasingly studied (e.g., Zaw, 1990, 2017; Cobbing et al., 1986, 1992; Gardiner et al., 2015a, 2015b, 2016a, 2016b, 2017; Jiang et al., 2017; Li et al., 2018; Li et al., 2018, 2019; Aung Zaw et al., 2017, 2021; Zhang et al., 2022; Mao et al., 2020, 2022). However, their geochemical characteristics, magma genesis, and tectonic settings are still not fully understood, especially in the southern part of the most Sn-rich central granitoid belt of Myanmar from Myeik to Kawthaung (Cobbing et al., 1986, 1992; Schwartz et al., 1995; Zaw et al., 2014). The aim of the investigation is to present detailed petrology, geochemistry, and geochronology of the granitic rocks between the Kawthaung and Bankachon area in the southernmost part of the Sn-related granitoid belt and discuss their petrogenesis, tectonic setting, and metallogenic implications.

2. General geology of the Kawthaung-Bankachon area

The Kawthaung-Bankachon area is located in the northern part of Kawthaung Township, Tanintharyi Region at the border of southern Myanmar and Thailand and about 19 km in E-W and 15 km in N-S direction with an aerial coverage of approximately 285 km^2.

* Corresponding author.
E-mail address: c.makoundi@utas.edu.au (C. Makoundi).

https://doi.org/10.1016/j.geogeo.2023.100188

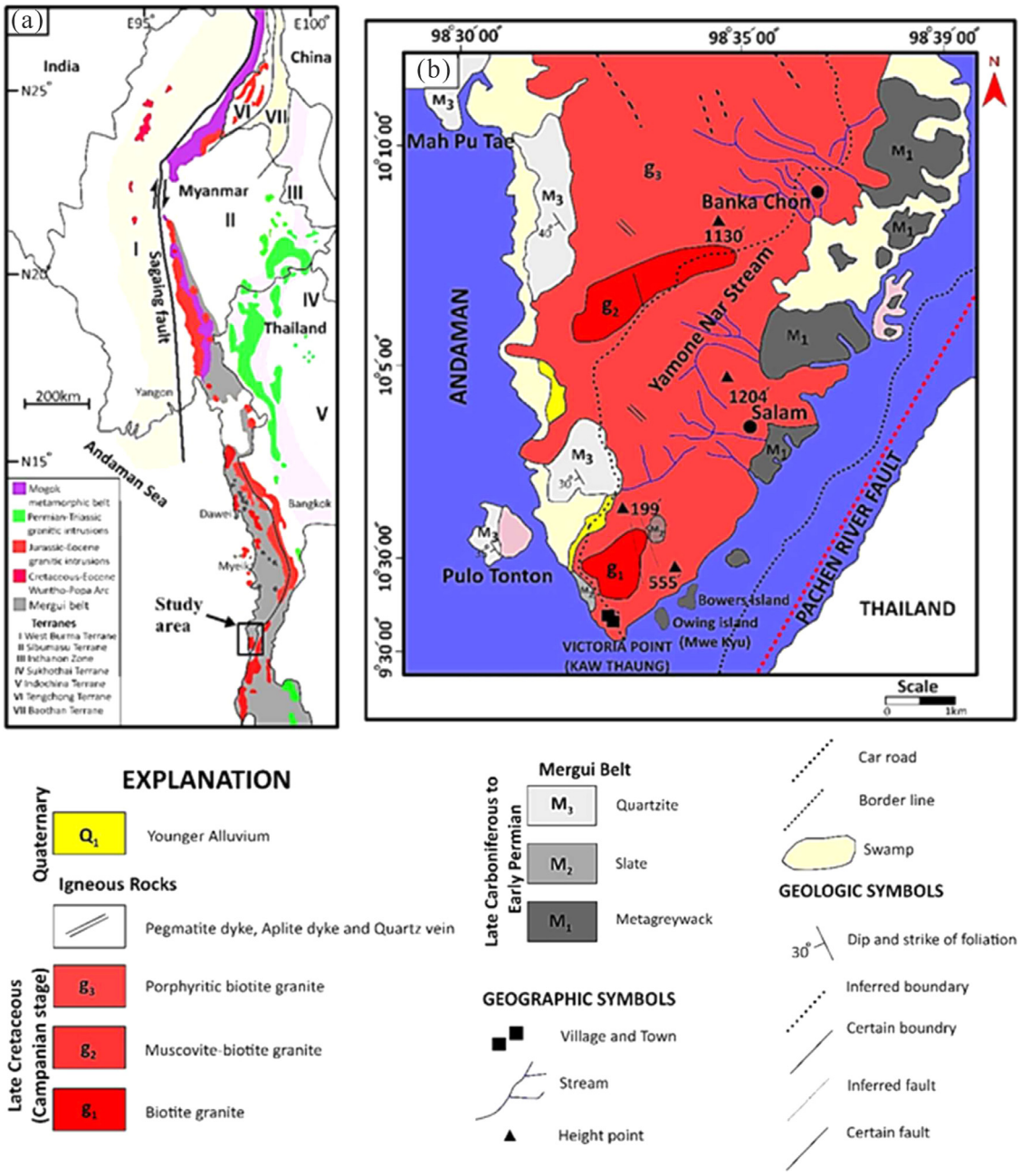

Fig. 1. (a) Regional setting of the granitoid belts in SE Asia (modified after Cobbing et al., 1986,1992; Zaw, 1990; Aung Zaw et al., 2021). (b) Detailed geological map of the area (after Zin, 2017, 2019, 2020; Zin Mar et al., 2019). Note granitoid of the studied area are located at the southernmost part of the W-Sn mineralization related to central granitoid belt of Myanmar.

The general geologic setting is shown in Fig. 1a and b. The middle part of the study area is higher in altitude than the eastern and western parts. The highest mountain range and the summits of the whole study area are found in the middle and northern parts of the area which is nearly NW-SE trending nine miles hill. It rises approximately 485 m (1590 ft) above sea level with the lowest mountain being approximately 169 m (555 ft). Many islands are distributed in the eastern, southern, and western parts of the study area.

In the regional framework, the area lies in the Shan-Tanintharyi area and the southern continuation of the Tanintharyi Ranges which belong to the western part of Sibumasu or Shan-Thai Block or Terrane. It also belongs to the western tin-bearing batholiths called the Western Tin Belt of Southeast Asia of Mitchell (1977); Thin (1984), and Cobbing et al. (1986, 1992) (Fig. 1a). The study area also falls within the Coastal Range Granite Belt of Brown and Heron (1923) stretching from southern Myanmar to Thai-Malay Peninsula. Brown and Heron (1923) described that these granitoids occur as three N-S trending subparallel belts: two of which, the eastern and central belts are documented in the Malay Peninsula, whereas the western belt is only exposed in western Thailand and Myanmar. The study area also corresponds to the southern part of the W-Sn mineralization related Central Granitoid belt of Zaw (1990, 2017) in which he described that the granitoids form a 1450 km long, narrow belt that is dominantly composed of calc-alkaline, peraluminous rocks. The granitic rocks intrude the Carboniferous Mergui Group which is unconformably underlain by gneisses and crystalline schists of probable Late Proterozoic or

Early Paleozoic age and being unconformably overlain by layers of limestone of Late Permian age, which is referred to as the Moulmein Limestone.

3. Methods of study

3.1. Field, sampling, and analytical whole rock XRF method

Fieldwork, including a systematic sampling of the representative rock units, measuring geological structures, and geological mapping have been carried out by using GPS (Global Positioning System). The geological data, which are collected from the field, are plotted on the quarter-inch topographic map. Modal analyses of the igneous rock units were made using the mechanical point counter in conjunction with the petrological microscope.

Quantitative and qualitative elemental analyses of various rock types have been carried out by using XRF technique studies. A total number of eleven representative samples of granitic rocks from the Kawthaung-Bankachon area have been selected and analyzed. All samples were sent to the geochemical and isotope laboratory of the Geological Survey of Japan, AIST. Samples of granitic rocks were analyzed by wavelength dispersive X-ray fluorescence (XRF) spectrometers, using the standard calibration method of AIST. The eighty grams of each crushed sample are ground by a variation mill. The sample containers of the mill are made of alumina. Plump samples are dried in an oven at 105°C for twenty-four hrs. The samples were heated in a Pt-Au crucible at 1250°C for seven minutes by a bead sampler. The trace elements and REEs were determined by Inductively Coupled Plasma Mass Spectrometry (ICP-MS). The results gave Fe_2O_3 as total iron.

3.2. LA ICP-MS U-Pb zircon geochronology

The representative samples collected from the Kawthaung to Bankachon area were analyzed in 2013-2014 by the U-Pb geochronology method using the LA-ICP-MS technique at the University of Tasmania, Australia. The LA-ICPMS method is now widely used for measuring U, Th, and Pb isotopic data (e.g., Fryer et al., 1993; Compston, 1999; Kosler and Sylvester, 2003; Black et al., 2003, 2004; Harley and Kelly, 2007). Approximately 100 g of rock was repeatedly sieved and crushed in a Cr-steel ring mill to a grain size <400 microns. The zircons were handpicked from the heavy mineral concentrates under the microscope in cross-polarized transmitted light. The selected crystals were placed on double-sided sticky tape and epoxy glue was then poured into a 2.5 cm diameter mould on top of the zircons. The mount was dried for 12 hours and polished using clean sandpaper and a clean polishing lap. The samples were then washed in distilled water in an ultrasonic bath.

The analyses in this study were performed on an Agilent 7500cs quadrupole ICPMS with a 193 nm Coherent Ar-F gas laser and the Resonetics M50 ablation cell. For each analysis, a subset of the data most closely matching a concordant composition has been selected for quantification. The downhole fractionation, instrument drift, and mass bias correction factors for Pb/U ratios were calculated using analyses of the 91500 zircon using values of Wiendenbeck et al. (1995). The instrument drift and mass bias correction factors for the $^{207}Pb/^{206}Pb$ ratio (ages) were calculated using analyses of the NIST610 glass, using the Pb isotopic values of Black et al. (2004). The calibration of the U-Pb ages was checked on analyses of the Temora zircon (Black et al., 2003) and Mud Tank zircon (Black and Gulson, 1978) analyzed throughout the analytical session and treated as unknowns. All common Pb corrections are done using Stacey and Kramer's (Stacey and Kramer, 1975) model Pb composition at the age of the zircon. The detailed data are listed in the Supplementary Data, Table S1.

Each analysis on the zircons began with a 30-second blank gas measurement followed by a further 30 seconds of analysis time when the laser was switched on. Zircons were sampled with 26–32-micron spots using the laser at 5 Hz and a density of approximately 2.1 J/cm^2. A flow of the carrier gas at a rate of 0.6 litres/minute carried particles ablated by the laser out of the chamber to be mixed with Ar gas and carried to the plasma torch. Isotopes measured include ^{49}Ti, ^{56}Fe, ^{90}Zr, ^{146}Nd, ^{178}Hf, ^{202}Hg, ^{204}Pb, ^{206}Pb, ^{207}Pb, ^{208}Pb, ^{232}Th, and ^{238}U with each element being measured every 0.16 s with a longer counting time on the U and Pb isotopes compared to the other elements. The data reduction used was based on the method outlined in detail in Meffre et al. (2008) similar to that outlined in Black et al. (2004) and Paton et al. (2010). Trace element abundances of zircons were calculated using the method outlined by Kosler (2001), using Zr as the internal standard element, assuming stoichiometric proportions, and using the NIST610 glass values of Jochum et al. (2011). Most of the selected zircon grains in the analyzed rocks are transparent and colorless under the microscope, although some appear brownish due to radiation damage from high U contents.

4. Characteristics of granitic rocks

The granitic rocks are mainly composed of biotite granite, muscovite-biotite granite, and porphyritic biotite granite. Pegmatite and aplite are formed as dykes (Zin Mar et al., 2019; Zin, 2017, 2019, 2020). Quartz veins and small diorite enclaves also occur. The metasedimentary rocks of the Mergui Group are quartzite, slate, and metagraywacke. Hornfels occur as small units at the contact zone of metasedimentary rocks and porphyritic biotite granite. The granitic rocks are classified and named based on modal analyses plotted on the IUGS classification diagram (Fig. 2). The lithological and textural characteristics of these units are described below.

4.1. Biotite granite

This unit is well-exposed in the southern part of the study area (Fig. 3a) and displays exfoliation weathering features and well-jointed nature. Orthoclase occurs as the most common feldspar, and some alter to sericite. The microcline is a subhedral form and shows cross-hatched twinning. Perthites are mainly of

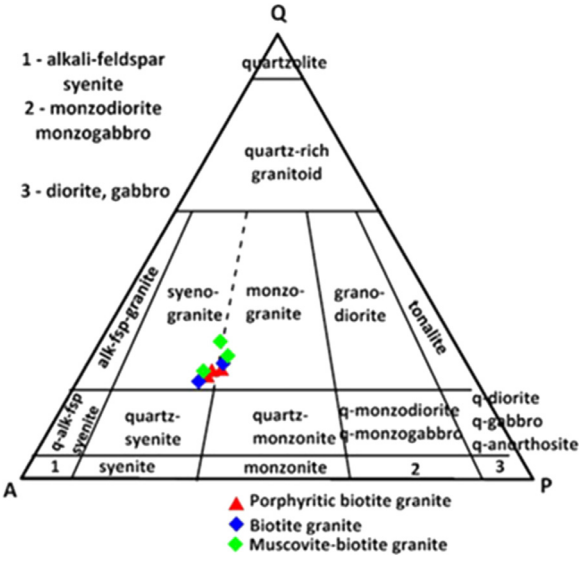

Fig. 2. Modal composition of the igneous rocks of the Kawthaung-Bankachon plotted on the IUGS classification diagram.

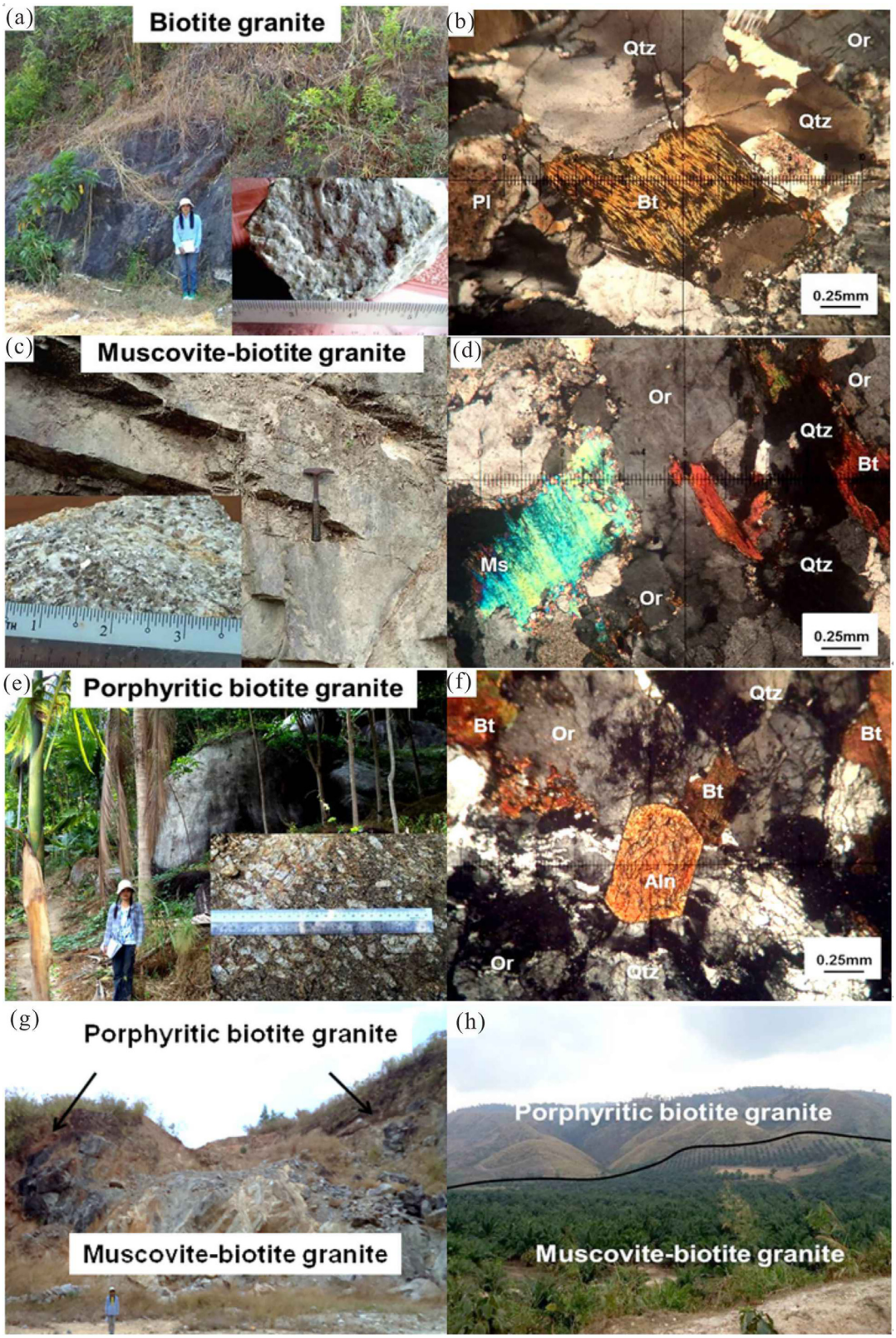

Fig. 3. Photographs and photomicrographs showing lithological characteristics of the Kawthaung-Bankachon area. (a) Outcrop nature of biotite granite unit. (b) Biotite altered to chlorite in biotite granite unit (between X.N) (Bt = biotite; Qtz = quartz; Or = orthoclase; Pl = plagioclase). (c) Horizontal jointed nature in muscovite-biotite granite unit. (d) Subhedral muscovite flake associated with orthoclase in muscovite-biotite granite unit (between X.N) (Ms = muscovite; Bt = biotite; Qtz = quartz; Or = orthoclase; Pl = plagioclase). (e) Prominent porphyritic biotite granite unit. (f) Zoning of euhedral allanite (Aln = allanite) in porphyritic biotite granite unit (between X.N) (Aln = allanite; Bt = biotite; Qtz = quartz; Or = orthoclase; Pl = plagioclase). (g) Contact of muscovite-biotite granite unit and porphyritic biotite granite unit. (h) Panoramic view of muscovite-biotite granite unit and porphyritic biotite granite unit.

flame perthite and micro string perthite. Closely spaced lamellae-polysynthetic twinning is recorded in plagioclase. The anorthite percentage of plagioclase feldspar determined by Michel's Levy method is An_3 to An_{19} (Albite to Oligoclase). Crystals are partially altered to sericite and saussurite along the twin planes. Most of the biotite is altered to chlorite along the margin and cleavage plane (Fig. 3b). Pleochroic haloes of zircon inclusions are also noted in biotite flakes.

4.2. Muscovite-biotite granite

The exposures of this unit are everywhere to be found in 12 miles Hill and 14 miles Hill Quarry. Most exposures are well jointed, especially horizontal jointed nature, and occur at Location N 10°07′48.9", E 98°34′02.3" (Fig. 3c). It also occurs as a sheet-like nature at Mee Kin Taung. The sharp contact of the intrusive muscovite-biotite granite and porphyritic biotite granite can be observed at Mya Kyauk Pwint Taung (Fig. 3g and h). Worm-like quartz is present along the plagioclase, giving rise to the myrmekitic texture. Micro string perthite is found under the microscope. Plagioclase composition is generally the An5-An12 (albite-oligoclase) range according to Michel Levy's method. Subhedral elongated muscovite flakes are associated with orthoclase (Fig. 3d).

4.3. Porphyritic biotite granite

At Chaung Salam monastery, porphyritic biotite granites are exposed as boulder nature (Fig. 3e). The sizes of phenocrysts are varying from 1-5 cm and vague foliation is visible in hand specimens. Patches of non-porphyritic biotite granite are found in some places. Some plagioclase twin bands are closely spaced. The compositional range is An_7-An_{15} (Albite-Oligoclase). The presence of myrmekitic quartz is closely associated with orthoclase feldspar. Most orthoclase is cloudy in appearance due to alteration of kaolinization and sericitization. Quartz occurs as anhedral irregular aggregates to lensoid elongated crystals. Biotite is strongly pleochroic with greenish brown to dark green due to chloritization. Some biotite flakes are bent and contorted. Elongation and zoning of euhedral alanites are observed in this unit (Fig. 3f). Secondary calcite vein intruded among the quartz grains. Contact of muscovite-biotite granite unit and porphyritic biotite granite unit can be observed at the Mya Kyauk Pwint Taung (Fig. 3g). At the top of 14 miles hill, a panoramic view of the muscovite-biotite granite unit and porphyritic biotite granite unit can be observed (Fig. 3h).

4.4. Pegmatite, aplite dykes, and quartz veins

The pegmatite dykes are found intruding into the porphyritic biotite granite. The general trends of the pegmatites are NE-SW and NW-SE directions. The average width of the pegmatite dyke is approximately 40 cm. It is mainly composed of quartz, orthoclase, muscovite, and tourmaline and locally is associated with cassiterite. Aplite dyke is also found intruding a quartzite unit which is trending approximately N-S. The average width of the aplite dyke is 15 cm. Quartz veins are found intruding the porphyritic biotite granite and biotite granite. Quartz veins have also been found in the granite by filling fissures probably related to the late-stage cooling of the magma. The general trends of quartz veins are in NW-SE directions.

4.5. Enclaves (Xenoliths)

Small diorite enclaves are quite common in porphyritic biotite granite. The diorite xenoliths are rounded in shape (about 10 cm in size) in the porphyritic biotite granite. The composition of plagioclase in diorite enclaves is An_{19}-An_{24} (oligoclase to andesine).

5. Geochemistry

5.1. Geochemical characteristics of granitic rocks

The Analytical data of major oxide, trace elements, and REE compositions are shown in Table 1. The granitic rocks in the study area are porphyritic biotite granite, biotite granite, and muscovite-biotite granite. Total alkali contents ($Na_2O + K_2O$) are 7.8-8.7 wt% with an average of 8.3 wt%. A/CNK (Molecular $Al_2O_3/(CaO + Na_2O + K_2O)$ is >1.1 for granitic rocks. In general, XRF geochemical analysis indicates SiO_2 (67.7-74.8 wt%), TiO_2 (0.09-0.69 wt%), Al_2O_3 (13.5-14.6 wt%), Fe_2O_3 as total iron (0.78-4.48 wt%), MnO (0.02-0.10 wt%), MgO (0.11-0.94 wt%), CaO (0.94-2.14 wt%), Na_2O (2.7-3.39 wt%), K_2O (4.74-5.53 wt%) and P_2O_5 (0.05-0.18 wt%). The bulk rock concentration of the granitic rocks is characterized by high SiO_2 and low MnO. TAS diagram, the sum of $Na_2O + K_2O$ (total alkali) vs. SiO_2 content which is the most useful preliminary classification of plutonic igneous rock after Middlemost (1985) is shown in Fig. 4. Accordingly, the granitic rocks in the study area fall in the granite fields. Variation diagrams of major element oxides and SiO_2 are used to interpret the behavior of elements in the magmatic fractionation. In Haker's (1909) variation diagram, major element oxides (Al_2O_3, TiO_2, MgO, MnO, Fe_2O_3, CaO and P_2O_5) against SiO_2 are negatively correlated, whereas the SiO_2 vs. Na_2O and SiO_2 vs. K_2O variation diagram show irregular scatter plots (Fig. 5). It suggests that the emplacement of the granitic rocks is likely due to the result of fractional crystallization during magmatic evolution.

The plot of the AFM diagram from Irvine and Baragar (1971) (A = ($Na_2O + K_2O$), F = Fe_2O_3 (as total iron), M = MgO) is shown in Fig. 6 which subdivides the sub-alkaline magma series to tholeiitic and calc-alkaline series and all samples fall in the calc-alkaline series. The SiO_2 vs K_2O plot after Peccerillo and Taylor (1976) of Fig. 7 shows that the granitic rocks of the study area fall in the high potassium calc-alkaline series and shoshonite series. In A/NK (molecular $Al_2O_3/Na_2O + K_2O$) vs. A/CNK (molecular $Al_2O_3/CaO + Na_2O + K_2O$) diagram (Fig. 8) after Shand (1943), the majority of the samples fall within the metaluminous to the slightly peraluminous field. The geochemical compositions of granitic rocks from the study area fall in the minor peraluminous and felsic aluminous fields of B = Fe + Mg + Ti vs. A = Al-(K + Na + 2Ca) diagram of Debon and Le Fort (1983) (Fig. 9). In

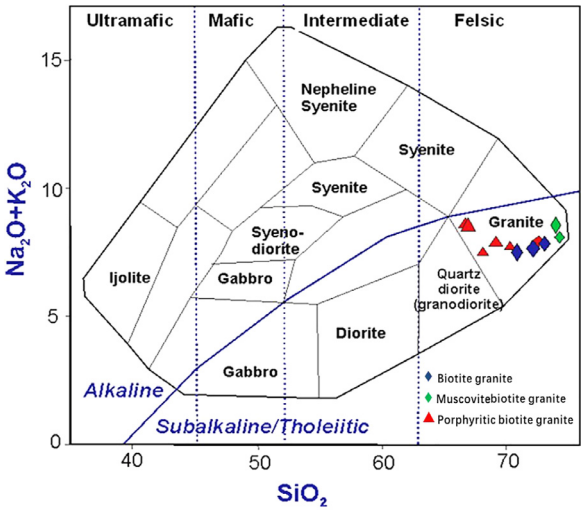

Fig. 4. Plot showing the granitic rocks from the Kawthaung-Bankachon area that falls in the granite field of classification of plutonic igneous rocks diagram after Middlemost (1985).

Table 1
Major, trace element and REE compositions of the granitic rocks of the Kawthaung-Bankachon area, southern Myanmar.

Sample	Biotite granite			Muscovite-biotite granite		Porphyritic biotite granite					
	Kt 2c	Kt 2d	Kt 2	Kt 3b	Kt 3	Kt 1a	Kt 1b	Kt 1c	Kt 1d	Kt 1g	Kt 1
Major element											
SiO_2 (wt %)	72.38	70.96	71.69	74.79	74.76	69.96	67.74	71.43	73.22	68.59	67.81
Al_2O_3	13.99	13.92	13.72	14.14	13.64	13.96	14.58	13.95	13.49	14.45	14.16
Fe_2O_3	2.689	3.142	2.95	0.927	0.782	3.686	4.208	2.955	2.475	4.233	4.476
CaO	1.425	1.929	1.584	0.939	0.665	2.1	2.006	1.826	1.466	2.137	2.119
MgO	0.383	0.607	0.537	0.125	0.112	0.724	0.746	0.566	0.318	0.788	0.939
Na_2O	3.143	2.877	3.125	3.262	2.853	2.888	3.394	2.864	3.168	2.97	2.698
K_2O	5.204	4.979	4.74	5.057	5.533	4.908	5.286	5.15	4.885	5.144	5.139
MnO	0.049	0.054	0.055	0.02	0.034	0.067	0.102	0.052	0.04	0.065	0.07
TiO_2	0.293	0.499	0.393	0.102	0.092	0.583	0.613	0.415	0.26	0.685	0.677
P_2O_5	0.075	0.111	0.091	0.045	0.068	0.125	0.158	0.097	0.064	0.162	0.179
LOI	0.59	1.07	0.51	0.045	0.88	1.08	0.67	1.00	0.74	0.62	0.53
Total	102.21	100.139	99.396	100.348	99.418	100.09	99.502	100.302	100.125	99.837	98.789
Trace element											
Ni (ppm)	<20	<20	<20	<20	<20	<20	<20	<20	<20	<20	<20
Cr	<20	<20	<20	<20	<20	<20	<20	<20	<20	<20	<20
W	<0.5	0.8	2.4	7.7	7	0.7	1.2	0.5	<0.5	0.7	3.2
V	10	16	23	<5	10	20	22	16	8	23	36
Ba	236	306	235	65	80	324	480	312	152	486	573
Rb	336	276	377	413	637	301	538	293	310	343	336
Sr	61	81	66	24	22	90	101	84	54	107	127
Zr	159	237	221	57	75	266	260	193	180	296	354
Y	20.9	51.3	50	24.8	28.2	61.8	33.9	36.7	17.1	43.1	46.1
Nb	10.6	19.5	17.3	13	34.3	21.3	18	14.2	9.5	17.9	20.2
Ga	19	19	22	22	26	21	23	20	19	20	23
Cu	<10	<10	<10	<10	<10	<10	<10	<10	<10	<10	<10
Zn	80	100	60	50	80	80	100	60	50	80	80
Pb	38	32	44	44	34	38	32	44	44	34	49
La	48.8	65.7	55.4	24.8	31	74.5	62.2	55	56.4	77.2	72.1
Ce	96.3	140	113	52.9	67.4	159	130	118	121	160	96.3
Th	60.6	71.5	63.3	23.2	34.7	84.5	49	66.6	73.6	67.4	63.4
Nd	38.9	59.2	47.7	20.1	26.2	65.5	53.5	48.2	46.3	66.5	63.1
U	9.97	14	15.2	18.5	21.1	16.9	5.87	14	14.6	8.43	7.74
Er	2.04	5.81	4.87	2.55	2.74	6.16	3.41	4.2	1.84	4.48	4.24
Gd	4.31	9.65	9.05	3.8	4.86	10.6	7.25	7.44	4.84	9.16	9.09
Hf	4.4	6.9	6.0	1.8	3.1	6.4	6.4	5.3	5.4	7.2	9.2
Th	60.6	71.5	63.3	23.2	34.7	84.5	49.0	66.6	73.6	67.4	63.4
Pr	11.2	16.0	13.1	5.87	7.66	17.9	14.8	13.3	13.3	18.3	17.1
Sm	6.56	12.1	9.98	4.39	6.22	13.2	9.79	9.04	7.84	12.1	11.8
Yb	2.23	5.81	4.64	2.59	2.88	5.73	3.07	4.19	2.05	3.85	3.82

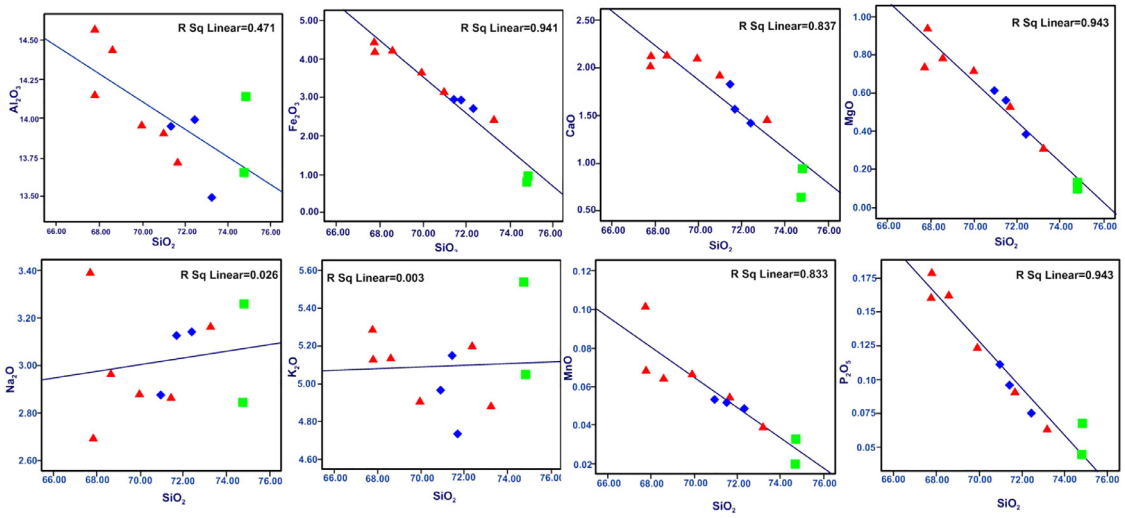

Fig. 5. Major oxide vs. SiO_2 Harker variation diagrams of the granitoid rocks of the Kawthaung-Bankachon area.

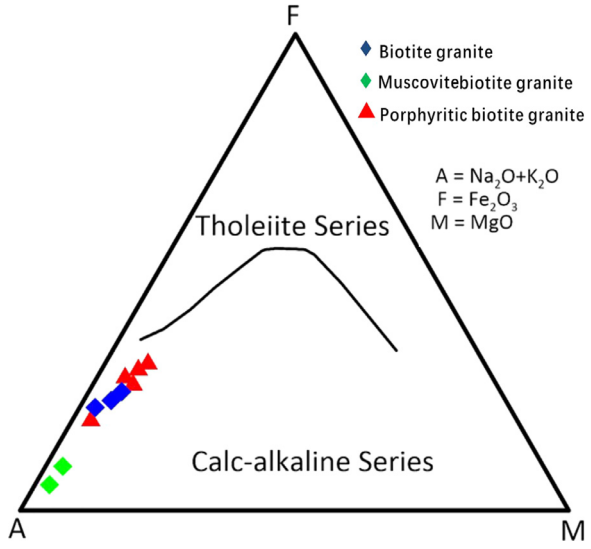

Fig. 6. AFM diagram indicates the subdividing of the sub-alkaline magma series to tholeiitic and calc-alkaline series after Irvine and Baragar (1971).

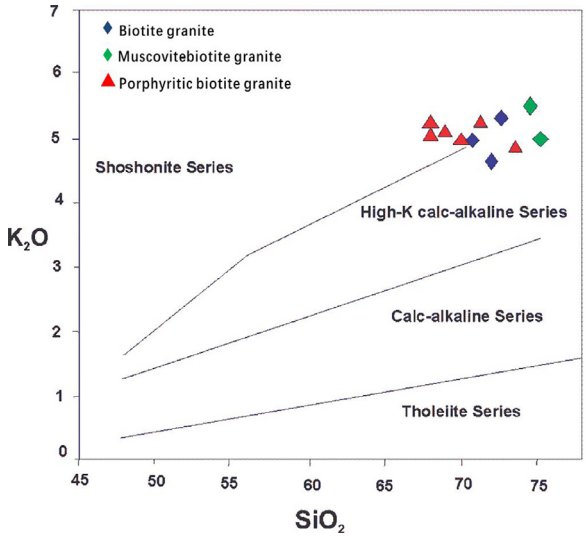

Fig. 7. SiO_2 vs. K_2O diagram showing high-calc-alkaline series to shoshonite series, according to Peccerillo and Taylor (1976).

the primitive mantle (Sun and McDonough, 1989) normalized trace elements spider diagram (Fig. 10), the granitic rocks are characterized by strong depletion of Ba, Sr, Nb, P and Ti and enrichment of Cs, Rb, U, Th, K, Pb, Nd, Zr, and Sm. REE distribution of the granitic rocks of the Kawthaung-Bankachon area shows a distinct depleted Eu anomaly (Fig. 11).

5.2. Genetic type of the granitic rocks

Major element characteristics of the granitic rocks are used as a key parameter for interpretation of the origin of granite. The scatter nature of the plots generated by major oxides, trace elements, and SiO_2 tends to indicate that they are of S-type (Chappell and White, 1974). The combined evidence including field observation, petrographic features, and geochemical characteristics of granite in the study area together with the occurrences of hornblende-bearing xenoliths (enclaves), biotite ± sphene, muscovite + biotite + hematite association, and the molecular $Al_2O_3/(CaO + Na_2O + K_2O)$ ratio of granite range 1.364-1.507 (>1.1) strongly indicate that the majority of granitic rocks

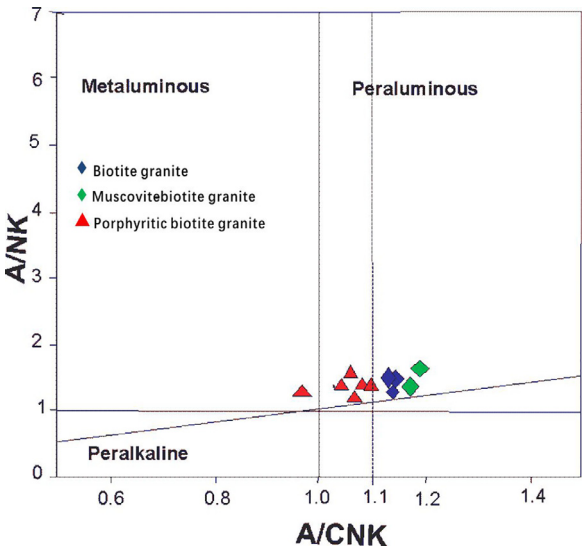

Fig. 8. A/NK (molecular Al_2O_3/Na_2O+K_2O) vs. A/CNK (molecular $Al_2O_3/CaO + Na_2O + K_2O$) diagram showing the peraluminous and metaluminous nature of the granitic rocks of the Kawthaung-Bankachon area after Shand (1943).

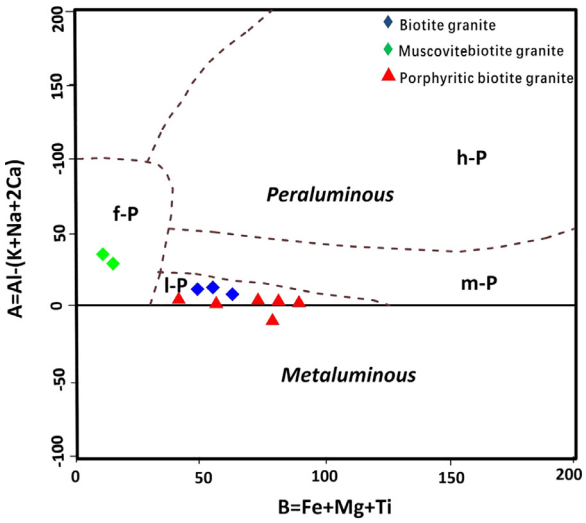

Fig. 9. B = Fe + Mg + Ti vs. A = Al-(K + Na + 2Ca) diagram of Debon and Le Fort (1983). Note granitic rocks from the Kawthaung-Bankachon area fall in peraluminous and felsic-peraluminous fields. f-P = felsic peraluminous; h-P = high peraluminous; m-P = moderately peraluminous; l-P = low peraluminous.

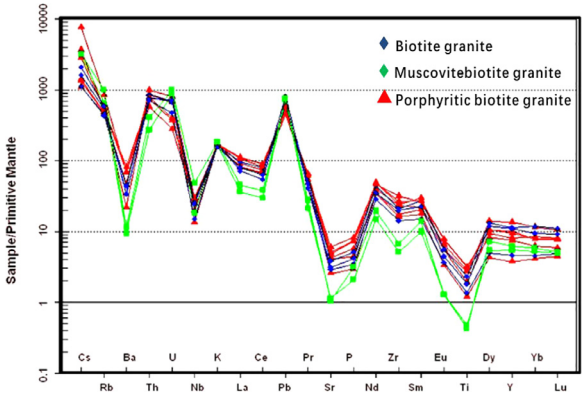

Fig. 10. Primitive mantle normalized trace elements multi-variation diagram for the granitic rocks of the Kawthaung-Bankachon area. Normalization values are from Sun and McDonough (1989).

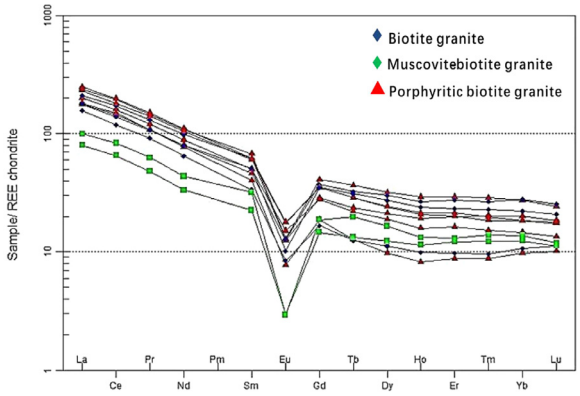

Fig. 11. REE distribution of the granitic rocks of the Kawthaung-Bankachon area. Note distinct depleted Eu anomaly.

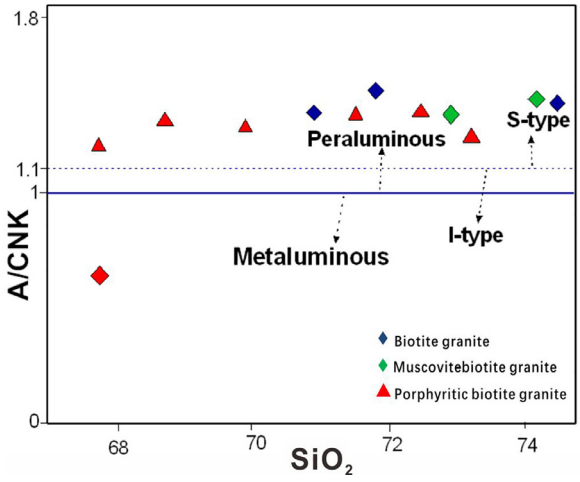

Fig. 12. SiO_2 vs. A/CNK (molecular $Al_2O_3/CaO + Na_2O + K_2O$) diagram for the granitic rocks of the Kawthaung-Bankachon area (after Chappell and White, 1974).

from the study area are S-type with the exception of porphyritic biotite granite (Chappell and White, 1974). The porphyritic biotite granite has $Al_2O_3/(CaO + Na_2O + K_2O)$ ratio of 0.007-0.0.503% (<1%) which shows the I-type feature.

The molecular A/CNK vs. SiO_2 diagram also shows that the majority of the granitic rocks from the study area involve S-type affinity with the exception of porphyritic biotite granite that falls to I-type affinity (Fig. 12; Chappell and White, 1974). This diagram defines A/CNK > 1.1 as S-type and A/CNK < 1.1 as I-type. According to the Na_2O vs. K_2O diagram, the granitic rocks belong to S-type affinity (Fig. 13; Chappell and White, 2001).

6. U-Pb zircon geochronology

The zircon grains with clear oscillatory zones were chosen for U–Pb dating. Porphyritic biotite granite (Kt. 1) that cropped out at Mee Kin Taung (Latitude 10°04′47.0" N, Longitude 98°32′31.3" E) gives the zircon age of 79.14 ± 0.91 Ma. Muscovite-biotite granite (Kt. 2) that cropped out at 12 miles Taung (Latitude 10°07′37.7" N 98°34′55.4", Longitude 98°32′31.3" E) yielded the zircon age of 79.59 ± 0.76 Ma. Biotite granite (Kt. 3) at 555 Taung (Latitude 10°08′47.0" N, Longitude 98°32′34.0" E) gives the zircon age of 78.97 ± 0.63 Ma. According to the age of zircon, the granitic rocks of the Kawthaung-Bankachon area are Campanian stage (Late Cretaceous). The Concordia plots for $^{238}U/^{206}Pb$-$^{207}Pb/^{206}Pb$ of separated zircon from granitic rocks at the Kawtaung to Bankachon area are shown in Figs. 14a, b and c, and U-Pb zircon age of the host granitoid rocks of the Yandapon Sn-W mine is shown in Fig. 14D). Table 2 shows LA ICP-MS zircon U-Pb age data of the Kawthaung-Bankachon area and Yadanabon Sn-W Mine, Myanmar.

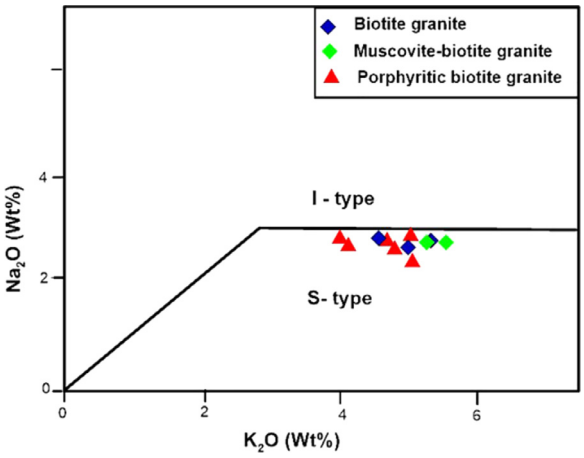

Fig. 13. Na_2O vs. K_2O diagram showing the mostly S-type and partially I-type nature of the granitic rocks of the Kawthaung-Bankachon area (after Chappell and White, 2001).

7. Discussion

7.1. Tectonic evolution of the Kawthaung-Bankachon granitoids

It was described that the granitic rocks in the Kawthaung-Bankachon area belong to the Central-Belt granitoids of Myanmar (Zaw, 1990, 2017). The Central-Belt granitoids of Myanmar corresponded to the Western granitoid Belt of Thailand (Charusiri, 1993; Charusiri et al., 1993). In a regional context, according to Cobbing et al. (1986, 1992), the central granitoid belt of Myanmar belongs to the Western Granite Province of the South-East Asia region. They mentioned that the Central belt granitic rocks of Myanmar were emplaced as early as the Jurassic but the bulk of granitoid intrusions in this belt was emplaced during the Late Cretaceous and Early Eocene.

The Central belt granitoids are considered to have been emplaced during the collision of the older magmatic-volcanic arc with the continental foreland to the east and these granitoid plutons are associated with tin-tungsten mineralization (Zaw, 1990, 2017). Cobbing et al. (1986, 1992) also described that the central granitoid belt of Myanmar includes both (I- and S-types) granites including the granitoid plutons of the Tanintharyi Region, and the plutons were successively emplaced during 85-59 Ma (Late Cretaceous to Paleocene). Cobbing (2011) further added that the Sibumasu terrane in Thailand was intruded by granite plutons of both S-type crustal origin and I-type mantle origin during the Late Cretaceous.

Searle et al. (2012) also recorded that Western Thailand–Myanmar/Burma province consists of hornblende–biotite I-type granodiorite–granites and felsic biotite–K-feldspar-muscovite- (± garnet ± tourmaline) and S-types granites associated with abundant tin mineralization in pegmatite dykes resulting from crustal thickening following the collision of the Sibumasu terrane with Indochina terrane. Similar I- and S-type granites are also recorded in Peninsular Malaysian granites (Ghani, 2005). In Thailand, the Eastern Granite Belt formed in the Early to Late Triassic (245-210 Ma), the Central Belt in Late Triassic to Middle Jurassic (220-180 Ma), and the Western Belt in the Late Cretaceous to Middle Tertiary (80-50 Ma) (Charusiri, 1993; Charusiri et al., 1993). Petrolog-

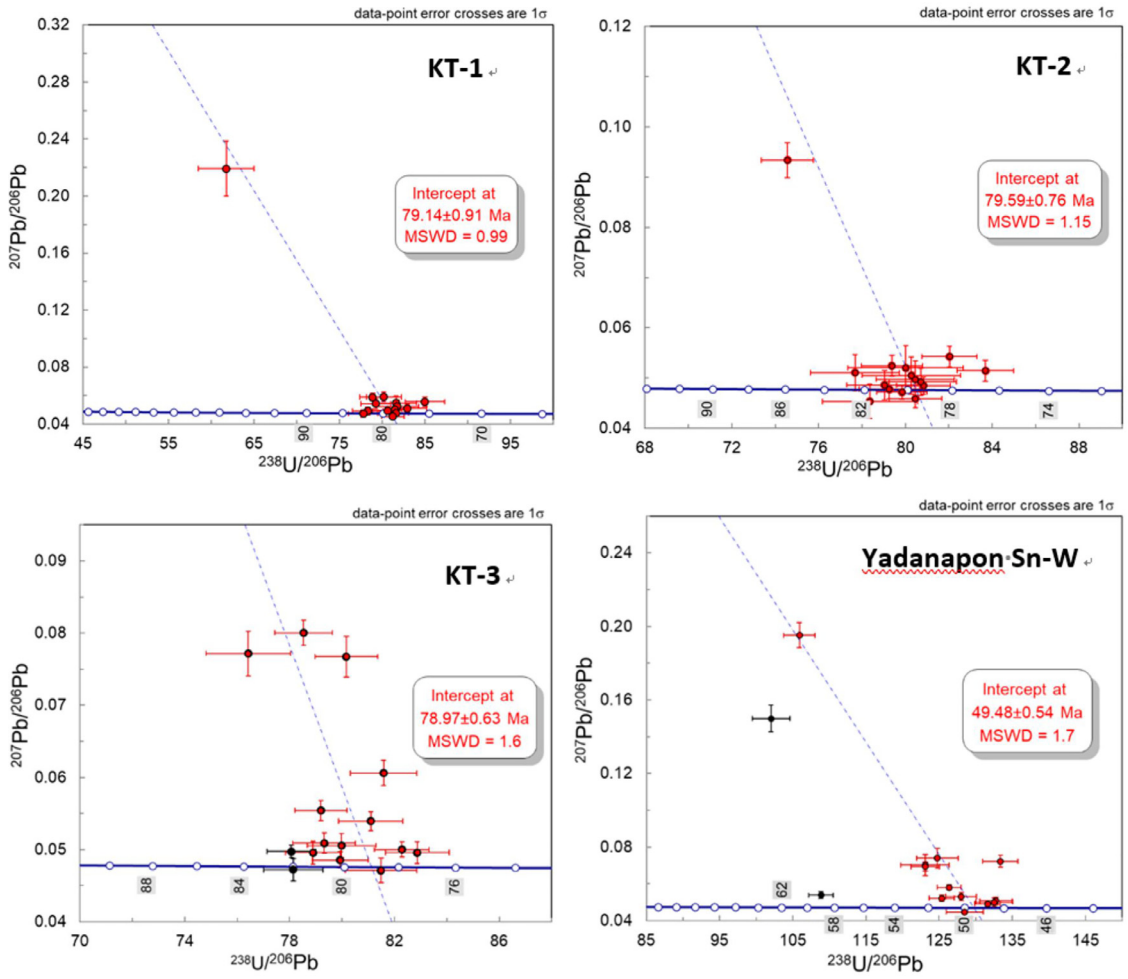

Fig. 14. (a) The Concordia diagram for $^{238}U/^{206}Pb$ - $^{207}Pb/^{206}Pb$ of separated zircon from biotite granite, (b) The Concordia diagram for $^{238}U/^{206}Pb$ - $^{207}Pb/^{206}Pb$ of separated zircon from muscovite- biotite granite and (c) The Concordia diagram for $^{238}U/^{206}Pb$ - $^{207}Pb/^{206}Pb$ of separated zircon from porphyritic biotite granite of the Kawthaung-Bankachon area.

Table 2
LA ICP-MS U-Pb Zircon age data of the Kawthaung-Bankachon area (Kt 1, Kt 2, and Kt 3) and Yadanabon Sn-W Mine, Myanmar.

Sample	Age (Ma)	±2s Uncertainty	±2s with* Systematic uncertainties	MSWD	Probability of fit	Number of analyses used for final age	Measured
KT-1	79.14	0.91	1.36	0.99	0.45	14	15
KT-3	79.59	0.76	1.27	1.15	0.31	15	15
KT-2	78.97	0.63	1.19	1.60	0.10	13	15
Yadanapon, Sn-W	49.48	0.54	0.83	1.70	0.06	12	15

* Systematic Uncertainties according to Horstwood et al. (2016). This uncertainty should be used when comparing with age estimates from other minerals, methods carried out in other laboratories.

ically, the Kawthaung-Bankachon granite does not contain hornblende, which is only found in the sedimentary enclaves, but with abundant muscovite. The color of alkali feldspar is pure white, and the occurrence of tin mineralization is also observed. The petrological characters of the granitic rocks in the study area are consistent with S-type granite. However, further about 159 km north from Kawthaung, especially at Karathuri tin-tungsten mine, both I-type and S-type granites occur. The configuration of the tectonic environment for the granitic rocks of the study area was investigated using the trivariate diagram of Rb/30-Hf-Tax3 (after Harris et al., 1986). The granitic rocks of the study area belong to syn-collision and late, post-collision settings (Fig. 15). When plotted on the trace element discrimination diagram (Pearce et al., 1984; Pearce, 1996), it is obvious that the granitic rocks from the Kawthaung-Bankachon area have tectonic affinities of post-collisional granite setting (Fig. 16).

7.2. Granite-related tin-tungsten mineralization in the Kawthaung-Bankchon and adjacent areas in Myanmar and Thailand

Granite-related tin-tungsten deposits widely occur in the Myanmar-Thailand border region (Fig. 17). This region is part of the globally important SE Asian tin belt which is accounted for 45% of the current world output of tin (Lehmann, 2021). For Myanmar, Gardiner et al. (2015b) pointed out that Myanmar can become the world's largest tin producer experiencing an increase in tin production in 2009-2014 up to 4900% due to the discovery of a new tin belt in Wa State, northern Myanmar. Despite recent upheaval and conflict in Myanmar, Myanmar and Thailand can become major producers of tin and tungsten in the longer term, especially through the development and renewed growth of the tin-rich southern part of the Myanmar-Thailand border region.

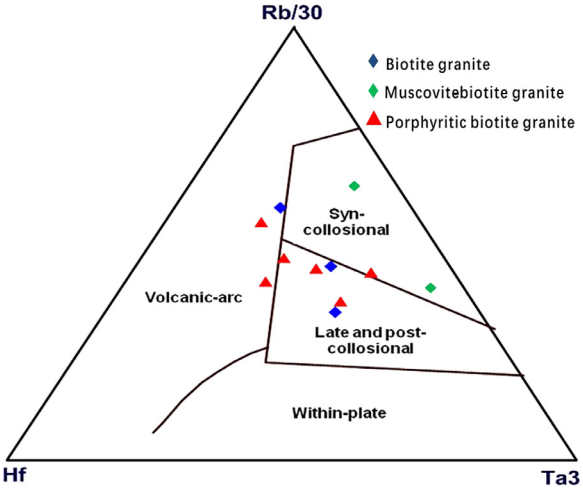

Fig. 15. Rb/30-Hf-Tax3 triangular plot showing the tectonic affinities of granitic rocks of the Kawthaung-Bankachon area (after Harris et al., 1986)

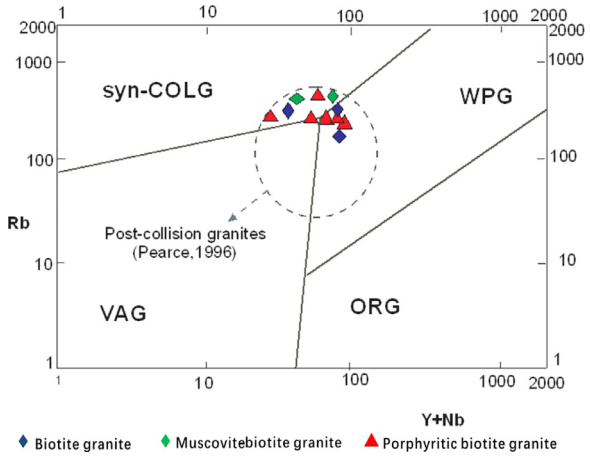

Fig. 16. Rb vs. (Y + Nb) diagram showing discrimination of the tectonic setting of granitic rocks of the Kawthaung-Bankachon area (after Pearce et al., 1984; Pearce et al., 1996).

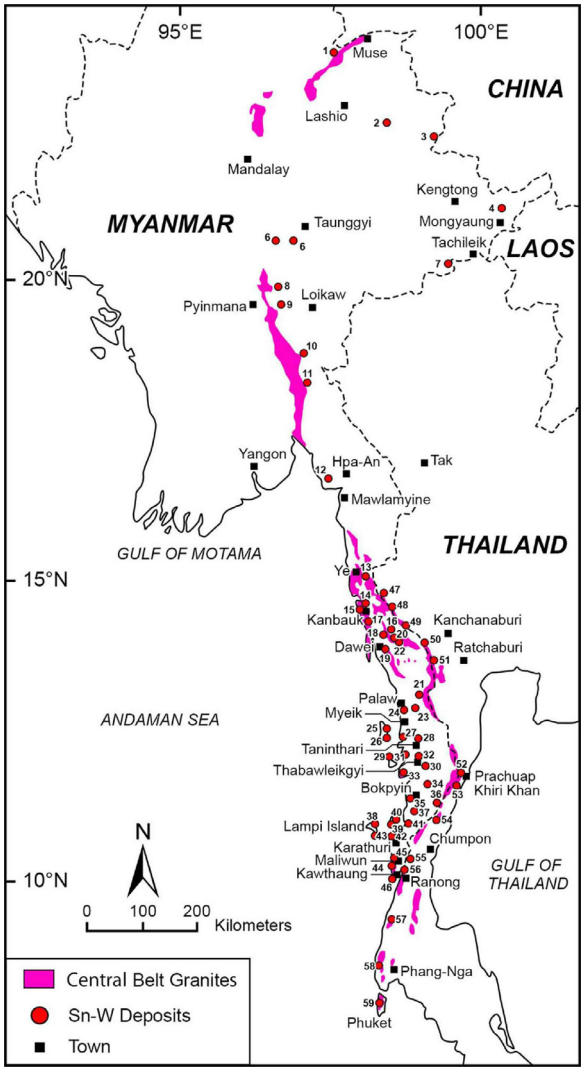

Fig. 17. Map showing Sn-W deposits along the Thailand-Myanmar border region. Tin–tungsten deposits of Myanmar. 1, Nam Kham; 2, Pansan–Pankhan; 3,Walinkhunmar; 4, Wan Pon; 5, Chaungnibauk; 6, Palamaw; 7, Mong Hsat; 8, Peinnedaik; 9, Myinmati; 10, Mawchi; 11, Mawday; 12, Natkyigyaung; 13,Natkyizin; 14, Ohnbinkwin; 15, Kanbauk; 16, Widnes; 17, Pha Chaung; 18, Hermyingyi; 19, Pagaye; 20, Mwehauk Chaung; 21, Nanthila; 22, Phachaung; 23,Thanbaya Chaung; 24, Palaw; 25, Yemyintkyi; 26, Yamon-kazat; 27, Zegami; 28, Gahan; 29, Dongyi; 30, Thabawleik; 31, Kadebyin; 32, Zalun; 33, Khe Chaung; 34, Yengan; 35, Bokpyin; 36, Yadanabon; 37, Kyaukhtanaung; 38, Lampi Island; 39, Harkapru; 40, Kyaukpan Chaung; 41, Chaungnagpi; 42,Karathuri; 43, Palau Bada; 44, Chockling; 45, Maliwun; 46, Pakchan River (modified after Than et al. 2017). Tin–tungsten deposits of Thailand: 47, Pilok; 48, Tao Dum; 49, Bong Ti; 50, Pu Nam Ron; 51, Takopidtong; 52, Nong Sue; 53, Tabsakae; 54, Salui; 55, Pajan; 56, Had Som Pan; 57, Ka Per; 58, Khao Lak; 59, Phuket (after Putthapiban and Gray, 1983; Putthapiban, 1984; Mahawat, 1984; Putthapiban, 1984; Charusiri, 1989; Charusiri et al., 1993; Nakapadungrat and Maneenai, 1993; Linnen et al., 1994; Department of Mineral Resource, 2007a, 2007b, 2008a, 2008b, 2013).

Than et al. (2017) reported that Sn-W deposits, mostly tin-rich, are widely distributed in the southern part of the Tanintharyi region, southern Myanmar. The most important Sn-W deposit is the Yadanabon Mine which is situated about 150 km northeast of Kawthaung. Tungsten (wolfram) and mixed concentrates are mined by lode mining of the quartz veins at the mine. There, a coarse-grained biotite–granite intruded into phyllites, slates, and quartzites of the Mergui Group (Carboniferous-Permian). Quartz veins and stringers penetrated both granite and sedimentary rocks. The size of these veins varies from 8-10 cm to 1 meter with Sn–W values higher in the thinner veins. The veins in the granite show greisenized borders. Pegmatites also occur in the area intruding the granite containing cassiterite. The quartz veins comprised wolframite, cassiterite, molybdenite, bismuth, bismuthinite, chalcopyrite, pyrite, tourmaline, and fluorite. Tin has also been mined from alluvium in the Namron Chaung area and there are prospective Sn–W areas to the north and south of the mine (Than et al., 2017). The Karathuri mine is about 160 km northeast of the study area and continuously extracting tin as a placer mining at present. The major granite-related tin mineralization is observed at about 32 km northeast of the study area, especially near Maliwun Village and cassiterite ores were extracted from the Maliwun tin deposit (10°14'N, 98°39'E). The area is located on the flank of the granite ranges which extend from Kawthaung to Talobusa. The tin mining operation in the area was in full swing during the Korean War. The large alluvial deposit that occurs at the foot of the hill produced 31 tons of tin concentrates in 1939 (Tin and Kyaw, 1966). The mine granite intruded the metasedimentary rocks of the Mergui Group. Quartz veins of different dimensions occur both in the granite and the sedimentary units. The ore minerals are wolframite, cassiterite, arsenopyrite, and pyrite.

Kyaw Thu et al. (2019) recently reported the occurrence of the Tagu tin–tungsten deposit which is one of the largest tin-tungsten deposits in the Myeik area, southern Myanmar. In the Tagu tin–tungsten deposit, nearly E–W trending vertical or steeply dipping

mineralized quartz veins are hosted by both Cretaceous to Eocene granite and Carboniferous to Early Permian metasedimentary rocks (Kyaw Thu et al., 2019). The host granitic rocks are composed of quartz, feldspars (plagioclase, orthoclase, and microcline), and micas (muscovite and biotite). They are S-type and peraluminous granite, formed in a syn-collisional setting. Mineralized veins at Tagu consist of early-formed oxide ore minerals, such as cassiterite and wolframite, which were followed by the formation of sulfide minerals.

The host granitoids of the Kawthaung-Bankachon area consist of a range of 65-573 ppm Ba. Barium substitutes for the K^+ ion and mainly occurs in K-feldspar and mica. In comparison, a variable amount of zircon (57-354 ppm) was recorded in the granitic rocks in the area, whereas yttrium presents a range of 17.1-61.8 ppm. The granitic rocks which have Sn content at or below the average value for the normal granitic rocks are tin-poor or barren plutons. Barsukov (1957) suggested that Sn-bearing granitic rocks contain 16-30 ppm Sn, whereas Sn-barren has 3-5 ppm. Beus and Grigorian (1977) indicated that mineralized or productive granitoids have 15 ppm Sn and barren or non-productive granitoids, have 5 ppm Sn. According to the trace element composition (Table 1), the granitic rocks of the study area contain 9-46 ppm Sn which shows the enrichment and mineralized nature of Sn if we compare it with the bulk continental crustal abundance of Sn which is only ~1.7 ppm (Rudnick and Gao, 2014).

Across the border from Myanmar into Thailand, tin mineralization is associated with the Phuket granitoids in southern Thailand (Fig. 17). Phuket is located 960 km southeast of Kawthaung, and there the tin mineralization is only associated with biotite muscovite ± tourmaline granites (SiO_2: 71.7 to 75.5 wt%) and low Sr and higher Rb content (Putthapiban, 1984). The granites are mainly S-type tin granites of Cretaceous ages (103 ± 6 to 78 ± 4 Ma) with minor amounts of I-type granites straddling the Myanmar-Thai border at least from the north, Tak to Kanchanaburi, through Pilok Sn-W mining district in Ranong to Khao Luk and Takua Pa in Phangnga to Phuket tin Island in the southwest of the Thai Peninsula (Fig. 17). Ranong is located just opposite of the study area, Kawthaung in Myanmar, just 300 km north of Phuket Island. One of the former largest Sn-W mines in southern Thailand, the Haad Som Pan mine is located in the Ranong Province, but mining operation is closed, and the area is now mined for kaolin as the major raw material products instead of rare metals, tin, and tungsten. The Maliwun mine in Myanmar used to extract tin by Government, but now only local people extract tin from this mine. The occurrences of tin mineralization in Kawthaung and its environs are both vein-type and placer-type. The tin-bearing granites in Kawthaung can be correlated with those from the Western granite province of Thailand.

The tin granites of western peninsular Thailand in general contain small to moderate batholiths and plutons of restricted composition (SiO_2: 68.4 to 75.5 wt%). Similar to those granites from the Eastern Belt Granites of Myanmar, in particular, the Kawthaung area, most of the Thai granites in this region intruded the Permo-Carboniferous pebbly rocks of Kaeng Krachan Formation (Putthapiban and Gray, 1983; Putthapiban, 2002, 2021; Putthapiban et al., 2019) which is equivalent to the Carboniferous-Permian Mergui Group of Myanmar.

The granites from both regions have shared many common lithological, petrographical, geochemical, and geochronological characteristics as well as their mineralization styles. However, the quantitative amounts of granite types may vary from area to area. At Ranong and Takua Pa, Phangnga area, coarse-grained porphyritic biotite granites are less predominant compared to those of the medium- to coarse-grained biotite–muscovite granites and the muscovite tourmaline granites. Muscovite and/or lepidolite-tourmaline pegmatite, aplite, and quartz veins are commonly observed in both granites and host country rocks of the Sn-W mineralized zone. For Phuket Island, four groups of granites, one I-type, and three S-types are recognized based on their field relations, petrographical, geochemical, and geochronological characteristics (Putthapiban and Gray, 1983; Putthapiban, 1984; Putthapiban, 2002, 2021; Putthapiban et al., 2019). The presence of a distinct mineral, allanite in the coarse-grained porphyritic biotite granites from both the Kawthaung study area and the Phuket area clearly indicated that the S-type granites from both areas were derived from a common or similar high aluminum and high REE crustal source rocks. At Phuket, only the S-type granites shown closely link to Sn-W mineralization. The tin granites, therefore, possess very strong crustal sources and fractionated signatures and high to very high initial $^{87}Sr/^{86}Sr$ ratios (0.7217 to 0.7438) which are, perhaps the characteristic of Sn-rich granites of these terrains in general.

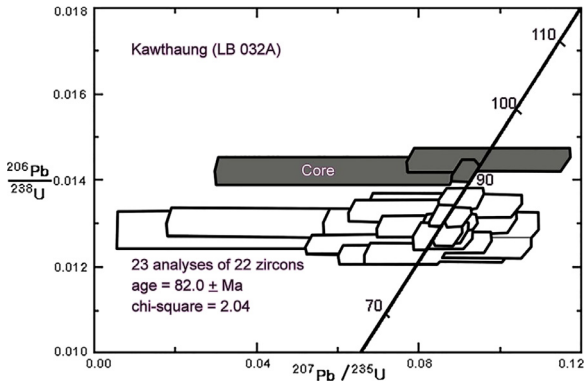

Fig. 18. Concordia diagram showing SHRIMP U-Pb in zircon data of the Kawthaung granitoid (Sample LB 032A) (after Pickard et al., 1996).

7.3. Geochronological constraints for tectonic evolution and timing of W-Sn metallogeny of the Kawthaung-Bankachon and adjacent area in SE Asia

The geochronological data in the Myanmar-Thai border region are shown in Table 3. The pioneering age determination studies of the southern Myanmar granitoids were undertaken by the Institute of Geological Sciences and British Geological Survey as early as 1970s and produced two important reports (Brook and Snelling, 1976) and compiled all age determinations in Myanmar by Zaw (2017). Darbyshire and Swainbank (1988) determined the ages of several granitoid intrusions in southern Myanmar using the $^{87}Sr/^{86}Sr$ method. The intrusions are from Davis Island, Pulo Baleigh, High Island, Parker and Trotter B Island, and Maingy Island including Auk Bok and Hermyingyi W-Sn deposit. They recorded $^{87}Sr/^{86}Sr$ age of 57 ± 4 Ma (Davis Island), 51 ± 13 Ma (Pulo Baleigh), 46 ± 16 Ma (High Island), 94 ± 14 Ma (Parker and Trotter B Island), 45±2 Ma (Maingyi island), 35 ± 34 Ma (Auk Bok) and 59 ± 2 Ma (Hermyingyi W-Sn deposit). The ages range from 35 ± 34 Ma at Auk Bok to 94 ± 14 Ma, at Parker and Trotter B Island. However, it should be noted that the Rb/Sr data are likely disturbed and reset due to later metamorphism and deformation. In comparison, the zircon U-Pb system has a relatively high closure temperature and is not easily disturbed by later thermal events. Pickard et al. (1996) recorded a U-Pb SHRIMP age of 82 ± 1.4 Ma for the Kawthaung granitoid and reanalysis of the Auk Bok and Hermyingyi granitoid samples by SHRIMP yielded 49.7 ± 0.5 Ma and 61.7 ± 1.3 Ma. The U-Pb Concordia diagram of the Kawthaung granitoid by the U-Pb SHRIMP method is shown in Fig. 18. The U-Pb SHRIMP age of 82 ± 1.4 Ma for the Kawthaung granitoid is consistent with the present U-Pb ICP-MS ages of the Kawthaung-

Table 3
The geochronological data in the Myanmar-Thai border region. LA ICP-MS U-Pb zircon radiometric age data of the Kawthaung-Bankachon area and Yadanabon Sn-W Mine and other published age data from Myanmar together with age data from near Pilok Mine, Pilok Sn-W Mine, Ranong, and Phuket-Phang Nga, southern Thailand. M=Muscovite; B=Biotite.

Location	Lithology	Age	Reference
Kawthaung-Bankachon, southern Myanmar	Porphyritic biotite granite, I-type	79.14±1.36 Ma (U-Pb LA ICP-MS)	this study
	Biotite granite, S-type	79.59±1.27 Ma (U-Pb LA ICP-MS)	this study
	Muscovite-biotite granite, S-type	78.97±1.19 Ma (U-Pb ICP MS)	this study
Kawthaung, southern Myanmar	Granite, S-type	82.0±1.4 Ma (U-Pb SHRIMP)	Pickard et al. (1996); Zaw (2017)
Kuntabin Sn–W deposit, Southern Myanmar	Two micas granites, S-type	90.1±0.7 Ma (U-Pb Zircon); 88.1±1.9 Ma (U-Pb (Cassiterite); 87.7±0.5 Ma (Re-Os molybdenite model age); 88.7±2.7 Ma (Re-Os Isochron age)	Mao et al. (2020)
Yadanabon Sn-W deposit, southern Myanmar	Granite, S-type	50.3 ±0.06 Ma (U-Pb LA ICP MS)	Gardiner et al. (2016a)
	Biotite granite, S-type	49.48±0.83 Ma (U-Pb LA ICP MS)	this study
Khao Daen granites, Kanchanaburi near Thai-Myanmar border	Biotite (-muscovite) granites, S-type	93±4 Ma (Rb/Sr isochron); 74±2 Ma (M. K/Ar); 71±2 Ma (B. K/Ar)	Beckinsale et al. (1979)
Khao Daen granites, Ban Phu Nam Ron, Kanchanaburi Province, Thailand-Myanmar border (Dawei)	Biotite granite, S-type	72 Ma (Ar-Ar)	Charusiri (1989) in Linnen and Williams Jones (1995)
Near Pilok Mine, western Thailand	Muscovite granite, S-type	74.4-76.5 Ma (Ar-Ar)	Charusiri (1989)
Pilok W-Sn Mine, western Thailand	Granitoids, S-type	73±3 Ma (M. K/Ar); 66±3 Ma (M. K/Ar); 63±9 Ma (B. K/Ar)	Burton and Bignell (1969)
Ranong, southern Thailand	Granitoids, S-type, Granites, S-type	72-87 Ma (Ar-Ar)	Charusiri et al. (1993)
		78±2 Ma (Rb/Sr isochron); 65±2 Ma (M. K/Ar)	Beckinsale et al. (1979)
Takua Pa-Phang Nga, southern Thailand	Granitoids, S-type	72-73 Ma, 55-58 Ma (Ar-Ar)	Charusiri et al. (1993)
Phang Nga-Phuket, southern Thailand	Granitoids, S-type	124±4, 108±5, 74±4 Ma (Rb/Sr isochrons)	Beckinsale et al. (1979)
Phuket, southern Thailand	Mainly S type with a single I-type pluton (82±4 Ma)	82±4, 98±7, 94±12, 84±1 Ma (Rb/Sr isochrons)	Putthapiban and Gray (1983)
	Mainly S-type with a single I-type pluton (82±4 Ma), Phuket Granites	82±4, 98±7, 100±6, 78±4 Ma (Rb/Sr isochrons)	Putthapiban (1984)
		61.5±5 Ma (M. K/Ar)	Pitakpaivan (1969)
		58±1.8, 57.4±1.5 Ma (M. K/Ar); 59.2±1.8, 55.8±1.7 Ma (B. K/Ar)	Bignell (1972)
		58.5 Ma (M. K/Ar); 55.4±2 Ma (B. K/Ar)	Garson et al. (1975)
		71.9±1, 70.9±1, 68.2±1 Ma (M. Rb-Sr); 55.2±0.6, 55.4±2, 56.6±0.6 Ma (B. Rb-Sr)	Putthapiban (1984)
		54.9±1.4, 82.3±1.0, 80.8±2.4 Ma (U-Pb ICP MS)	Charusiri and CODES University of Tasmania in Morley (2012)

Bankachon area (78.97 ± 0.63, 79.59 ± 0.76 and 79.14 ± 0.91 Ma). Li et al. (2019) reported U-Pb zircon ages of several granitoid plutons in southern Myanmar ranging from 74 ± 0.3 Ma to 83.9 ± 0.5 Ma and their ages are consistent with our age data of the Kawthaung-Bankachon area. We also recorded 49.48 ± 0.83 Ma for the host biotite granite from the Yadanabon W-Sn deposit which is similar to the U-Pb age of 50.3 ± 0.06 Ma for the granite reported by Gardiner et al. (2016a).

In terms of timing for the Sn-W mineralization in southern Myanmar, Mao et al. (2020) reported a zircon U-Pb age of 90.1 ± 0.7 Ma for the two-mica granite and cassiterite U-Pb age of 88.1 ± 1.9 Ma at the Kuntabin W-Sn deposit in the Mergui (Myeik) area near the Tagu Mine (Kyaw Thu Kyaw Thu et al., 2019), north of the Kawthaung-Bankachon area. They also provided Re-Os weighted mean model age of 87.7 ± 0.5 Ma and an isochron age of 88.7 ± 2.7 Ma for the molybdenite in the Kuntabin deposit and indicated a clear genetic relationship between granite and Sn-W mineralization in the deposit and implied the earliest ~90 Ma magmatism and Sn-W mineralization in the Sibumasu and Tengchong terranes related to subduction of the Neo-Tethys oceanic subduction.

Mao et al. (2022) reported U-Pb ages of cassiterite grains from the primary W-Sn deposits in and around the Tavoy (Dawei) area, more than 200 km further north of the Kawthaung-Bankachon area: Pagaye (71.5 ± 0.7 Ma), Bwabin (63.3 ± 0.6 Ma), Hermyingyi (61.2 ± 1.3 Ma), and Mawchi (43.1 ± 0.8 Ma). Zhang et al. (2022) also conducted U-Pb age analysis of various cassiterite, and wolframite samples and recorded from 60.4 ± 0.9 Ma to 69 ± 0.5 Ma with the exception of 84.9 ± 0.5 Ma for one sample. Their samples are from the different mines and prospects mostly from the Tavoy (Dawei) district such as Hermyingyi, Thitkhatoe, Thaling Taung, Kalonta, Taungphila, Pagaye, Bawapin, Kanbauk, and Letha Taung which are further north of the Kawthaung-Bankachon area.

LA-ICP-MS U-Pb dating of zircon from the host biotite granite at the world-class Hermyingyi W-Sn deposit (Khin Myo Thet, 1983; Aung Zaw et al., 2017) yielded U–Pb ages of 61.44 ± 0.6 Ma (Li et al., 2018), 70.44 ± 0.4 Ma (Jiang et al., 2017) and molybdenite Re-Os isochron age of 68.4 ± 2.5 Ma (Jiang et al., 2019). The LA-ICP-MS U-Pb zircon age of the biotite granite from Taungphila near Hermyingyi was dated 68.8 ± 0.1 Ma (Jiang et al., 2017). Li et al. (2018) recorded U-Pb cassiterite ages of 60.7 ± 2.5 Ma and 62.5 ± 1.0 Ma at Bawabin and 64 ± 3.9 Ma at Kalonta near Hermyingyi. Li et al. (2018) provided a U–Pb zircon age of 60.7 ± 3.5 Ma and Re-Os molybdenite age of 64.5 ± 3.7 Ma at the W-Sn Wagone deposit which is consistent with the Re-Os molybdenite age of 60 ± 2.5 Ma, 64.6 ± 3.9 Ma, and 68.4 ± 2.5 Ma) which were reported by Aung Zaw et al. (2021). Combining all the U-Pb zircon age of host rocks and mineralization ages by cassiterite and molybdenite, it is likely that the age of ~60 Ma is the significant metallogenic timing for the W-Sn mineralizing event in the Tavoy (Dawei) district, southern Myanmar.

Aung Zaw et al. (2021) studied the timing of W-Sn formation in the Padatgyaung region in central Myanmar and recorded two weighted average Re-Os model ages of 64.23 ± 0.29 Ma and 60.54 ± 0.45 Ma from vein molybdenites and considerably older molyb-

denite from tin mineralized greisen which has a weighted Re-Os model age of 68.5 ± 2.7 Ma.

Aung Zaw et al. (2017) recorded a U-Pb zircon age of 42.72 ± 0.94 Ma for the host granite at the world-class Mawchi W-Sn deposit and Re-Os molybdenite age of 42.4 ± 1.2 Ma for the mineralization age. The age of the host granitoid was supported by the recent U-Pb age of 43.1 ± 0.8 Ma by Mao et al. (2022). In this study, we recorded a U-Pb zircon age of 49.48 ± 0.54 Ma for the host granitoid at the Yadanapon W-Sn deposit just 10 km north of the Kawthaung-Bankachon area. Although further work on the timing of mineralization is required, it is imperative to consider that ~40-45 Ma is also an important W-Sn mineralization event in southern Myanmar.

Across the border from Myanmar to southern Thailand, radiometric dating of granitoid was initially undertaken by Pitakpaivan (1969), Burton and Bignell (1969), Bignell (1972), Garson et al. (1975), Backinsale et al. (1979), Putthapiban and Gray (1983) and Putthapiban (1984) using K-Ar, Ar-Ar and Rb-Sr methods and recently by Charusiri and CODES University of Tasmania listed in Morley (2012) using LA ICP MS U-Pb zircon method (Table 3).

Beckinsale et al. (1979) recorded K-Ar age of 71 ± 2 and 74 ± 2 Ma and Rb-Sr isochron age of 93 ± 4 Ma for Khao Daen S-type granites, Ban Phu Nam Ron, Kanchanaburi Province, Thailand-Myanmar border (Dawei). In comparison, Charusiri (1989) reported Ar-Ar age of 72 Ma for the Khao Daen S-type granites. For the Ranong S-type granite in southern Thailand just next to the Kawthaung-Bankachon area, K-Ar age of 65 ± 2 Ma, Rb/Sr isochron age of 78 ± 2 Ma, and Ar/Ar age of 72-78 Ma are reported (Beckinsale et al., 1979; Charusiri et al., 1993). Further north, Charusiri et al. (1993) yielded Ar-Ar ages of 55-58 Ma to 72-73 Ma for the granitoids from Takua Pa-Phang Nga, southern Thailand. Several age determinations were conducted for various granitoid units in Phuket Island and K-Ar ages of 55.4 ± 2 Ma – 61.5 ± 5 Ma were reported (Pitakpaivan, 1969; Bignell, 1972; Garson et al., 1975; Backinsale et al., 1979). In comparison, Putthapiban and Gray (1983) and Putthapiban (1984) largely recorded Rb-Sr ages of 55.2 ± 0.6 Ma – 78 ± 4 Ma to 94 ± 12 Ma – 100 ± 6 Ma for the S-type granitoid units and 82 ± 4 Ma for I-type granitoid unit. In the Phang Nga area, Backinsale et al. (1979) also reported up to Rb-Sr age of 124 ± 4 Ma. In contrast, U-Pb zircon ages of 54.9 ± 1.4 Ma, 82.3 ± 1.0 Ma, and 80.8 ± 2.4 Ma are reported by Charusiri and CODES University of Tasmania for the Phuket granitoid.

For the Pilok W-Sn deposit in Thong Phaphum, Kanchanaburi, western Thailand, Burton and Bignell (1969) first reported K-Ar ages of 63 ± 9 Ma – 73 ± 3 Ma of the host granite and Charusiri (1989) yielded Ar-Ar age of 72 Ma on biotite from granite 8 km northwest of the Pilok deposit and 74.4-76.5 Ma for the muscovite intergrown with cassiterite and wolframite in a quartz vein. The Pilok W-Sn deposit is located 50 km north of the Hermyingyi W-Sn deposit in the Dawei area, southern Myanmar (Lemann et al., 1994; Linnen and William-Jones, 1995). Both deposits are large-scale primary granite-related vein-greisen deposits occurring in the apical zone of aplogranite intrusions. Although further timing for W-Sn mineralization at the Pilok deposit is warranted, the 60 Ma mineralization event is considered in the western and southern Thailand territory.

On this basis, the U-Pb zircon ages together with the geological, petrological, and geochemical characteristics, are suggestive that the tectonic setting, magmatism, and W-Sn mineralization in the southern Myanmar-western Thailand were mainly attributable to India Oceanic subduction, and collision between the west Myanmar terrane and the Sibumasu terrane during the Late Cretaceous. A petrogenetic and metallogenic model related to the tectonic setting of granitic rocks of the study area is shown in Fig. 19.

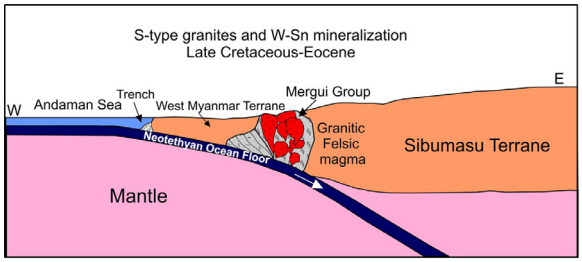

Fig. 19. Tectonic and W-Sn metallogenic model for the granitic rocks of the Kawthaung- Bankachon area, southern Myanmar (modified after Sanemasu et al., 2014).

8. Conclusions

The Kawthaung-Bankchon area lies in the southernmost part of Myanmar adjacent to western Thailand. This area occurs in the Shan-Tanintharyi Block of the Eastern Highland of Sibumatsu terrane and forms part of the W-Sn-related Central Granitoid Belt of Myanmar which belongs to the Western tin-bearing batholiths or Western Tin Belt of Southeast Asia tin-tungsten provinces. The granitoid units in the area are biotite granite, muscovite-biotite granite, porphyritic biotite granite, and diorite which sometimes occur as dykes, and they are characterized by a high-K calc-alkaline series and belong to the peraluminous field. In the molecular A/CNK vs. A/NK diagram, the majority of the granitic rocks in the study area fall in S-type affinity but some porphyritic biotite granites are slightly akin to I-type affinity. According to the tectonic discrimination diagram, the granitic rocks are clearly in the syn- to post-collisional granite field.

U-Pb Zircon age determination of the granitic rocks in the area recorded ages of 78.97 ± 0.63 Ma (biotite granite), 79.59 ± 0.76 Ma (muscovite-biotite granite), and 79.14 ± 0.91 Ma (porphyritic biotite granite) and were emplaced during the Campanian stage (Late Cretaceous). In comparison, 49.48 ± 0.83 Ma is recorded for the host biotite granite from the Yadanabon W-Sn deposit. The magmatism and W-Sn mineralization in the Kawthaung-Bankchon area encompassing the Thai and Myanmar region are mainly attributable to oceanic subduction and the collision between the west Myanmar terrane and the Sibumasu terrane during the Late Cretaceous to Paleogene.

Declaration of Competing Interest

The authors declare that they have no known competing financial interests or personal relationships that could have appeared to influence the work reported in this paper.

CRediT authorship contribution statement

Zin Mar Oo: Conceptualization, Formal analysis, Writing – original draft. **Khin Zaw:** Supervision, Writing – review & editing, Validation. **Ivan Belousov:** Methodology, Writing – original draft. **Prinya Putthapiban:** Writing – review & editing, Resources. **Charles Makoundi:** Writing – review & editing, Validation, Resources.

Acknowledgements

The authors are indebted to all staff members of the Economic Geology Lab., Department of Earth Resources Engineering, Kyushu University, Japan for their supporting XRF analysis for this work. The authors thank U Than Htun for his constructive discussion. The authors are greatly thankful to Prof Santosh for his suggestion and

reading of the earlier version of the manuscript. The handling editor and the reviewers are highly appreciated for their constructive and useful comments to improve the manuscript.

Supplementary materials

Supplementary material associated with this article can be found, in the online version, at doi:10.1016/j.geogeo.2023.100188.

References

Aung Zaw, Myint, Khin, Zaw, Ye Myint, Swe, Yonezu, K., Cai, Y., Manaka, T., Watanabe, K., 2017. Geochemistry and geochronology of granites hosting the Mawchi Sn-W deposit, Myanmar: implications for tectonic setting and granite emplacement. In: Barber, A.J., Crow, M.J., Khin, Zaw (Eds.), Myanmar: Geology, Resources and Tectonics. Geological Society, London, Memoirs, pp. 385–400 48.

Aung Zaw, Myint, Huan, Li, Mitchell, A.H.G., Selby, D., Wagner, T., 2021. Geology, mineralogy, ore paragenesis, and molybdenite Re-Os geochronology of Sn-W (-Mo) mineralization in Padatgyaung and Dawei, Myanmar: implications for timing of mineralization and tectonic setting. J. Asian Earth Sci. 212 (2021), 104725.

Barsukov, V.L., 1957. The geochemistry of tin. Geochemistry 1, 41–52.

Beckinsale, R.D., Suensilpong, S., Nakapadungrat, S., Walsh, J.N., 1979. Geochronology of granite magmatism in Thailand in relation to a plate tectonic model. J. Geol. Soc. London 136, 529–540.

Beus, A.A., Grigorian, S.V., 1977. Geochemical Exploration Methods for Mineral Deposits. Applied Publishing, Wilmette.

Bignell, J.D., 1972. The Geochronology of the Malayan Granites Ph.D. Thesis. University of Oxford, UK.

Black, L.P., Gulson, B.L., 1978. The age of the mud tank carbonatite, strangways range, Northern Territory. BMR J. Australian Geol. Geophys. 3, 227–232.

Black, L.P., Kamo, S.L., Allen, C.M., Aleinikoff, J.N., Davis, D.W., Russell, J., Korsch, R.J., Foudoulis, C., 2003. TEMORA 1: a new zircon standard for phanerozoic U-Pb geochronology. Chem. Geol. 200 (1-2), 155–170.

Black, L.P., Kamo, S.L., Allen, C.M., Davis, D.W., Aleinikoff, J.N., Valley, J.W., Mundil, R., Campbell, I.H., Korsch, R.J., Williams, I.S., Foudoulis, C., 2004. Improved $^{206}Pb/^{238}U$ microprobe geochronology by the monitoring of a trace-element related matrix effect; SHRIMP, ID-TIMS, ELA-ICP-MS, and oxygen isotope documentation for a series of zircon standards. Chem. Geol. 205, 115–140.

Brook, M., Snelling, N.J., 1976. K:Ar and Rb:Sr age determinations on rocks and minerals from Burma. Institute of Geological Sciences, London, Geochemical Division, Isotope Geology Unit, Report 76/12.

Brown, J.C., Heron, A.M., 1923. The geology and ore deposits of Tavoy District. Memoir Geol. Survey India 44, 167–354.

Burton, C.K., Bignell, J.D., 1969. Cretaceous-tertiary events in Southeast Asia. Bull. Geol. Soc. Am. 80 (4), 681–688.

Chappell, B.W., White, A.J.R., 1974. Two contrasting granite types. Pacific Geology 8, 173–174.

Chappell, B.W., White, A.J.R., 2001. Two contrasting granite types: 25 years later. Austr. J. Earth Sci. 48, 489–499.

Charusiri, P., Clark, A.H., Farrar, E., Archibald, D., Charusiri, B., 1993. Granite belts in Thailand: evidence from the $^{40}Ar/^{39}Ar$ geochronological and geological syntheses. J. Southeast Asian Earth Sci. 8, 127–136.

Charusiri, P., 1989. Lithophile Metallogenic Epochs of Thailand: A Geological and Geochronological Investigation. Queen's University, Kingston, Canada, p. 819 Unpublished Ph.D. thesis.

Cobbing, E.J., Mallick, D.I.J., Pitfield, P.E.J., Teoh, L.H., 1986. The granites of the Southeast Asian Tin belt. J. Geol. Soc. London 143, 537–550. doi:10.1144/gsjgs.143.3.0537.

Cobbing, E.J., Pitfield, P.E.J., Derbyshire, D.P.F., Mallick, D.I.J., 1992. The granites of the South-east Asian Tin Belt. Overseas Memoir of the British Geological Survey 10. HMSO, London.

Cobbing, E.J., 2011. Chapter 16: Granitic rocks. In: Ridd, M.F., Barber, A.J., Crow, M.J. (Eds.), The Geology of Thailand. Geological Society, London, pp. 459–492.

Compston, W., 1999. Identifying granite sources by SHRIMP U-Pb zircon geochronology: an application to the Lachlan fold belt. Contrib. Mineral. Petrol. 37, 323–341.

Debon, F., Le Fort, P., 1983. A chemical-mineralogical classification of common plutonic rocks and associations. Trans. R. Soc. Edinburgh 73, 135–149. doi:10.1017/S0263593300010117.

Department of Mineral Resources, 2007a. The Subdivision for Geological and Geologic Resources Management of Chumphon Province, Department of Mineral Resources. Ministry of Natural Resources and Environment, Bangkok, p. 68 (in Thai.

Department of Mineral Resources, 2007b. The Subdivision for Geological and Geologic Resources Management of Ranong Province, Department of Mineral Resources. Ministry of Natural Resources and Environment, Bangkok, p. 63 (in Thai).

Department of Mineral Resources, 2008a. The Subdivision for Geological and Geologic Resources Management of Kanchanaburi Province, Department of Mineral Resources. Ministry of Natural Resources and Environment, Bangkok, p. 96 (in Thai.

Department of Mineral Resources, 2008b. The Subdivision for Geological and Geologic Resources Management of Prachuap Khiri Khan Province, Department of Mineral Resources. Ministry of Natural Resources and Environment, Bangkok, p. 102 (in Thai).

Department of Mineral Resources, 2013. The Subdivision for Geological and Geologic Resources Management of Phang Nga Province, Department of Mineral Resources. Ministry of Natural Resources and Environment, Bangkok, p. 121 (in Thai).

Fryer, B.J., Jackson, S.E., Longerich, H.P., 1993. The application of laser ablation microprobe-inductively coupled plasma-mass spectrometry (LAM-ICP-MS) to in situ U & Pb geochronology. Chem. Geol. 109 (1-4), 1–8.

Gardiner, N.J., Searle, M.P., Robb, L.J., Morley, C.K., 2015a. Neo-Tethyan magmatism and metallogeny in Myanmar-an Andean analogue? J. Asian Earth Sci. 106, 197–215.

Gardiner, N.J., Sykes, J.P., Trench, A., Robb, L.J., 2015b. Tin mining in Myanmar: production and potential. Res. Policy 46, 219–233.

Gardiner, N.J., Robb, L.J., Morley, C.K., Searle, M.P., Cawood, P.A., Whitehouse, M.J., Kirkland, C.L., Roberts, N.M.W., Tin Aung, Myint, 2016a. The tectonic and metallogenic framework of Myanmar: a Tethyan mineral system. Ore Geol. Rev. 79, 26–45.

Gardiner, N.J., Searle, M.P., Morley, C.K., Whitehouse, M.P., Spencer, C.J., Robb, L.J., 2016b. The closure of Palaeo-Tethys in Eastern Myanmar and Northern Thailand: new insights from zircon U-Pb and Hf isotope data. Gondwana Res. 39, 401–422.

Gardiner, N.J., Hawkesworth, C.J, Robb, L.J., Whitehouse, M.J., Roberts, N.M.W., Kirkland, C.L., Evans, N.J., 2017. Contrasting granite metallogeny through the zircon record: a case study from Myanmar. Sci. Rep. 7, 748.

Garson, M.S., Young, B., Mitchell, A.H.G., Tait, B.A.R., 1975. The geology of the tin belt in peninsular Thailand around Phuket, Pangnga and Takua Pa. In: Overseas Mem. No. 1. I.G.S., London, p. 112.

Ghani, A.A., 2005. Geochemical characteristic of S- and I-type granites: example from Peninsular Malaysia granites. Geol. Soc. Malaysia Bulletin 123–134.

Harker, A., 1909. The natural history of igneous rocks. Methuen & Co., London.

Harley, S.L., Kelly, N.M., 2007. The impact of zircon-garnet REE distribution data on the interpretation of zircon U-Pb ages in complex high-grade terrains: an example from the Rauer Islands. East Antarctica. Chem. Geol. 214, 62–87.

Horstwood, M.S.A., Košler, J., Gehrels, G., Jackson, S.E., McLean, N.M., Paton, C., Pearson, N.J., Sircombe, K., Sylvester, P., Vermeesch, P., Bowring, J.F., Condon, D.J., Schoene, B., 2016. Community-derived standards for LA-ICP-MS U-(Th-)Pb geochronology – uncertainty propagation, age interpretation and data reporting. Geostand. Geoanal. Res. 40 (3), 311–332. doi:10.1111/j.1751-908X.2016.00379.x.

Irvine, T.N., Baragar, W.R.A., 1971. A guide to the chemical classification of the common volcanic rocks. Can. Jour. Earth. Sci. 8, 523–548.

Jiang, H., Li, W.Q., Jiang, S.Y., Wang, H., Wei, X.P., 2017. In: Geochronological, geochemical and Sr-Nd-Hf isotopic constraints on the petrogenesis of Late Cretaceous A-type granites from the Sibumasu Block, 268–271. Southern Myanmar, SE Asia, Lithos, pp. 32–47.

Jiang, H., Jiang, S.Y., Li, W., Zhao, K., 2019. Timing and source of the Hermyingyi W-Sn deposit in Southern Myanmar, SE Asia: Evidence from molybdenite Re-Os age and sulfur isotopic composition. J. Earth Sci. 30, 70–79.

Jochum, K.P., Weis, U., Stoll, B., Kuzmin, D., Yang, Q., Raczek, I., Jacob, D.E., Stracke, A., Birbaum, K., Frick, D.A., Gunther, D., Enzweiler, J., 2011. Determination of reference values for NIST SRM 610–617 glasses following ISO guidelines. Geostand. Geoanal. Res. 35, 397–429.

Kosler, J., Sylvester, P.J., 2003. Recent trends and the future of zircon in geochronology: laser ablation ICPMS. Mineral. Geochem. 53 (1), 243–275.

Kosler, J., 2001. Laser-ablation ICPMS study of metamorphic minerals and processes. In: Sylvester, P.J. (Ed.), Laser-Ablation-ICPMS in the Earth Sciences; Principles and Applications. Mineral Association of Canada Short Course Handbook, pp. 185–202 29.

Kyaw Thu, Htun, Yonezu, K., Myint, Aung Zaw, Tindell, T., Watanabe, K., 2019. Petrogenesis, ore mineralogy, and fluid inclusion studies of the Tagu Sn–W deposit, Myeik, Southern Myanmar. Minerals 9, 654. doi:10.3390/min9110654.

Lehmann, B., Jungyusuk, N., Khositanont, S., Hohndorf, A., Kuroda, Y., 1994. The tin–tungsten ore system of Pilok, Thailand. J. Southeast Asian Earth Sci. 10, 51–63.

Lehmann, B., 2021. Formation of tin ore deposits: A reassessment. Lithos 402-403, 105756.

Li, H., Myint, Aung Zaw, Yonezu, K., Watanabe, K., Algeo, T.J., Wu, J-H., 2018. Geochemistry and U–Pb geochronology of the Wagone and Hermyingyi A type granites, southern Myanmar: implications for tectonic setting, magma evolution and Sn–W mineralization. Ore Geol. Rev. 95, 575–592.

Li, J.X., Fan, W.M., Zhang, L.Y., Evans, N.J., Sun, Y.L., Ding, L., Guan, Q.Y., Peng, T.P., Cai, F.L., Sein, K., 2019. Geochronology, geochemistry and Sr–Nd–Hf isotopic compositions of Late Cretaceous-Eocene granites in southern Myanmar: petrogenetic, tectonic and metallogenic implications. Ore Geol. Rev. 112, 103031.

Linnen, R.L., Williams-Jones, A.E., 1995. Genesis of a magmatic metamorphic hydrothermal system: the Sn-W Polymetallic Deposits at Pilok, Thailand. Econ. Geol. 90, 1148–1166.

Mahawat, C., 1984. The geological characteristics of the Pilok Sn-W-Mo deposits, West Thailand. In: International Symposium on the Geology of Tin Deposits. Naning, China, pp. 95–108 26th-30th October 1984.

Mao, W., Zhong, H., Yang, J.H., Tang, Y.W., Liu, L., Fu, Y., Zhang, X.C., Sein, K., Aug, S.M., Li, J., Zhang, L., 2020. Combined zircon, molybdenite, and cassiterite geochronology and cassiterite geochemistry of the Kuntabin tin-tungsten deposit in Myanmar. Econ. Geol. 115 (3), 603–625.

Mao, W., Zhong, H., Yang, J.H., Liu, L., Fu, Y., Zhang, X.C., Tang, Y., Li, J., Zhang, L., Sein, K., Aung, S.M., Paw, S.M.T.L., Doh, S.H., 2022. Geochronology of Sn mineralization in Myanmar: metallogenic implications. Econ. Geol. doi:10.5382/econgeo.4927, ISSN 0361-0128.

Meffre, S., Large, R.R., Scott, R., Woodhead, J., Chang, Z., Gilbert, S.E., Danyushevsky, L.V., Maslennikov, V., Hergt, J.M., 2008. Age and pyrite Pb-isotopic composition of the giant Sukhoi Log sediment-hosted gold deposit, Russia. Geochim. Cosmochim. Acta 72, 2377–2391.

Middlemost, E.A.K., 1985. Magmas and Magmatic Rocks. An Introduction to Igneous Petrology. Longman, London, New York.

Mitchell, A.H.G., 1977. Tectonic settings for emplacement of Southeast Asia tin granites. Geol. Soc. Malaysia Bull. 9, 124–140.

Morley, C., 2012. Late cretaceous–early Palaeogene tectonic development of SE Asia. Earth Sci. Rev. 115, 37–75.

Nakapadungrat, S., Maneenai, D., 1993. The Phuket Phangnga and Takua Pa Tin-Field Thailand. J. Asian Earth Sci. 8, 359–368.

Nyan, Thin, 1984. Some Aspects of Granitic Rocks of Tenasserim Division (Unpublished) Dept. of Geology. University of Yangon, Myanmar.

Paton, C., Woodhead, J.D., Hellstrom, J.C., Hergt, J.M., Greig, A., Maas, R., 2010. Improved laser ablation U–Pb zircon geochronology through robust downhole fractionation correction. Geochem. Geophys. Geosyst. 11, 1–36. doi:10.1029/2009GC002618.

Pearce, J.A., Harris, N.W., Tindle, A.G., 1984. Trace elements discrimination diagrams for tectonic interpretation of granitic rocks. J. Petrol. 25, 956–983.

Pearce, J.A., 1996. Sources and setting of the granitic rocks. Episodes 19, 956–983.

Peccerillo, A., Taylor, S.R., 1976. Geochemistry of Eocene Calc-alkaline volcanic rocks from the Kastamonu area, Northern Turkey. Contrib. Mineral. Petrol. 58, 63–81.

Pickard, A.L., Barley, M.E., Zaw, Khin, 1996. Zircon SHRIMP Ages for a Selection of Granites from Myanmar. Unpublished report, Key Centre for Strategic Mineral Deposits. Department of Geology and Geophysics, University of Western Australia, Nedlands, p. 6907 Australia.

Pitakpaivan, K., 1969. Tin-bearing and tin-barren granite in Thailand. In: Proc. 2nd Tech. Conf. on Tin. International Tin Council, Bangkok, I, pp. 283–298.

Putthapiban, P., Gray, C.M., 1983. Age and tin-tungsten mineralization of the Phuket granites. In: Thailand. Paper presented at the Conference on Geology and Mineral Resources of Thailand, 19-28th November 1983, Bangkok, Thailand, pp. 30–39.

Putthapiban, P., Chao, Lin, Cho Aye, Cho, Paik, Mi, Nualkhao, P., Salyapongse, S., 2019. Granite magmatism and related mineralization in Thailand: Implications for the Thai Myanmar Border Region. In: Abstract Vol., Second International Conference on Applied Earth Sciences in Myanmar and Neighboring Regions (MAESA), 29/30 November-1 December 2019. Novotel Hotel, Yangon, Myanmar, p. 26.

Putthapiban, P., 1984. Geochemistry, Geochronology and Tin Mineralization of Phuket granites, Phuket, Thailand. Ph.D. Thesis. La Trobe University, Victoria, Australia.

Putthapiban, P., 2002. In: Mantajit, Nopadon (Ed.), Geology and Geochronology of Thailand, the Symposium of the Geology of Thailand, Bangkok, Thailand, pp. 261–283.

Putthapiban, P., 2021. Granite geology of western Thailand and the related mineralization. In: Program and Abstract Vol., Geothai Webinar, p. 91 4-6 August 2021.

Rudnick, R.L., Gao, S., 2014. Composition of the continental crust. In: Holland, H.D., Turekian, K.K. (Eds.), Treatise on Geochemistry 3. Elsevier, Amsterdam, pp. 1–51.

Sanematsu, K., Manaka, T., Zaw, K., 2014. Geochemical and geochronological characersistics of granites and Sn-W-REE mineralisation in the Tanintharyi region, southern Myanmar. 2nd Regional Congress on Geology, Mineral and Energy Resources of Southeast Asia Abstract Vol..

Schwartz, M.O., Rajah, S.S., Askury, A.K., Putthapiban, P., 1995. The Southeast-Asian Tin Belt. Earth Sci. Rev. 38, 95–286.

Searle, M.P., Whitehouse, M.J., Robb, L.J., Ghani, A.A., Hutchison, C.S., Sone, M., Ng, S.W.-P., Roselee, M.H., Chung, S.-L., Oliver, G.J.H., 2012. Tectonic evolution of the Sibumasu–Indochina terrane collision zone in Thailand and Malaysia: constraints from new U–Pb zircon chronology of SE Asian tin granitoids. J. Geol. Soc. 169, 489–500.

Shand, S.J., 1943. Eruptive rocks. Their Genesis, Composition, Classification, and their Relation to Ore Deposits. John Wiley & sons, New York, p. 488.

Stacey, J.S., Kramers, J.D., 1975. Approximation of terrestrial lead isotope evolution by a two-stage model. Earth Planet. Sci. Lett. 26, 207–221. doi:10.1016/0012-821X(75)90088-6.

Than, Htun, Than, Htay, Zaw, Khin, 2017. Tin–tungsten deposits of Myanmar. In: Barber, A.J., Zaw, Khin, Crow, M.J. (Eds.), Myanmar: Geology, Resources and Tectonics. Geological Society, London, Memoirs, pp. 625–647. doi:10.1144/M48.28.

Tin, Aye, Kyaw, Nyein, 1966. Review of Tin and Tungsten Deposits of Burma. First Burma Research Congress, Rangoon, Burma, pp. 39–73.

Wiedenbeck, M., Allé, P., Corfu, F., Griffin, W.L., Meier, M., Oberli, F., von Quadt, A., Roddick, J.C., Spiegeln, W., 1995. Three natural zircon standards for U-Th-Pb, Lu-Hf, trace element and REE analysis. Geostandards Newsletter 19, 1–23.

Zaw, Khin, Myo Thet, Khin, 1983. A note on a fluid inclusion study of tin-tungsten mineralization at Mawchi Mine, Kayah State. Burma. Econ. Geol. 78, 530–534.

Zaw, Khin, Meffre, S., Lai, C.K., Burrett, C., Santosh, M., Graham, I., Manaka, T., Salam, A., Kamvong, T., Cromie, P., 2014. Tectonics and metallogeny of mainland Southeast Asia — a review and contribution. Gondwana Res 26, 5–30.

Zaw, Khin, 1990. Geological, Petrological and Geochemical Characteristics of Granitiod Rocks in Burma; with Special Reference to the Associated W-Sn mineralization and their tectonic setting. Jour. SE Asian Earth Sci. 4, 293–335.

Zaw, Khin, 2017. Overview of mineralization styles and tectonic-metallogenic setting in Myanmar. In: Barber, A.J., Zaw Khin & Crow, M.J. (Eds) Myanmar: Geology, Resources and Tectonics. Geological Society, London, Memoirs, 48, 531–556, 10.1144/M48.24.

Zhang, Q., Zhao, K-D., Li, W-Q., Palmer, M.R., Jiang, S-Y., Jiang, H., Wei Zhang, W., Zhang, D., Hussain, A., 2022. Timing and tectonic setting of tin mineralization in southern Myanmar: constraints from cassiterite and wolframite U–Pb ages. Miner. Deposita doi:10.1007/s00126-021-01083-y.

Zin Mar, Oo, Thompson, J., Zaw, Khin, 2019. Tectonic Setting of the rocks in the Kawthaung Area, southernmost part of Myanmar: Constraints from Petrology, geochemistry and U-Pb zircon geochronology. Abstract Vol., Second International Conference on Applied Earth Sciences in Myanmar and Neighboring Regions (MAESA). Novotel Hotel, Yangon, Myanmar 29/30 November-1 December 2019.

Zin Mar, Oo, 2019. Petrography and petrochemical analyses of rocks along the contact zone between country rocks and granitic rocks from Bankachon Area, Kawthaung Township, Tanintharyi Region, southernmost part of Myanmar: Constraints for their tectonic exhumation and U-Pb zircon age. Abstract Vol., 3rd International Conference on Substantial Scientific Collaborations of Ocean and Earth Science Between Myanmar and China (SSCOE). West Yangon University, Yangon, Myanmar November 2019.

Zin Mar, Oo, 2020. Study on the genetic type and rare earth elements in the Kawthaung Area, Tanintharyi Region. Myanmar. Abstract Vol., 4th Myanmar National Conference on Earth Sciences (MNCES), 28-29 December 2020. Taungoo University, Taungoo, Myanmar.

Zin, Mar Oo, 2017. Petrological and geochemical analyses of the rocks between Kawthaung-Bankachon area, Tanintharyi Region. PhD thesis. University of Yangon, Myanmar.